NAVAL POSTGRADUATE SCHOOL

MONTEREY, CALIFORNIA

THESIS

FRICTION STIR PROCESSING OF AS-CAST AA5083: SUPERPLASTIC RESPONSE

by

John Toshio Hayashi

June 2009

Thesis Advisor:	Terry R. McNelley
Co-Advisor:	Jianqing Su
	Sarath Menon

Approved for public release; distribution is unlimited

THIS PAGE INTENTIONALLY LEFT BLANK

REPORT DOCUMENTATION PAGE			Form Approved OMB No. 0704-0188
Public reporting burden for this collection of information is estimated to average 1 hour per response, including the time for reviewing instruction, searching existing data sources, gathering and maintaining the data needed, and completing and reviewing the collection of information. Send comments regarding this burden estimate or any other aspect of this collection of information, including suggestions for reducing this burden, to Washington headquarters Services, Directorate for Information Operations and Reports, 1215 Jefferson Davis Highway, Suite 1204, Arlington, VA 22202-4302, and to the Office of Management and Budget, Paperwork Reduction Project (0704-0188) Washington DC 20503.			
1. AGENCY USE ONLY *(Leave blank)*	**2. REPORT DATE** June 2009	**3. REPORT TYPE AND DATES COVERED** Master's Thesis	
4. TITLE AND SUBTITLE Friction Stir Processing of As-Cast AA5083: Superplastic Response		**5. FUNDING NUMBERS**	
6. AUTHOR(S) John Toshio Hayashi			
7. PERFORMING ORGANIZATION NAME(S) AND ADDRESS(ES) Naval Postgraduate School Monterey, CA 93943-5000		**8. PERFORMING ORGANIZATION REPORT NUMBER**	
9. SPONSORING /MONITORING AGENCY NAME(S) AND ADDRESS(ES) N/A		**10. SPONSORING/MONITORING AGENCY REPORT NUMBER**	
11. SUPPLEMENTARY NOTES The views expressed in this thesis are those of the author and do not reflect the official policy or position of the Department of Defense or the U.S. Government.			
12a. DISTRIBUTION / AVAILABILITY STATEMENT Approved for public release; distribution is unlimited		**12b. DISTRIBUTION CODE** A	

13. ABSTRACT (maximum 200 words)

Plates of continuously cast AA5083 were subjected to friction stir processing (FSP) by three overlapping plunge and traverses. The FSP used a threaded pin tool with a pin diameter of 3 mm, pin length of 3 mm and a shoulder diameter of 10 mm. The process was run at constant tool rotation and traverse speeds of 800 rpm and 76.2 mm min^{-1}, respectively. The microstructure of the processed region was examined by optical microscopy and orientation imaging microscopy. FSP of the AA5083 reduced the average grain size from approximately 60 μm in the base metal to 3-4 μm in the processed zone. In addition, it created a homogeneous microstructure and, in particular, a refined and homogenous particle distribution without damage to the particles. Large tensile samples with gage sections of 1x3x8 mm were prepared by wire EDM for high-temperature tension testing. Tensile tests were carried out at 450°C under different strain rates. The relationship between strain rate and elongation was established. A maximum superplastic elongation of ~550% was obtained at a strain rate of 3×10^{-3} s^{-1}. The formation mechanism of refined grain structure and the superplastic characteristic of FSP material will be discussed in this paper

14. SUBJECT TERMS Friction Stir Processing, Superplasticity, Elevated Temperature, Aluminum, Grain Refinement, Strain Rate			**15. NUMBER OF PAGES** 67
			16. PRICE CODE
17. SECURITY CLASSIFICATION OF REPORT Unclassified	**18. SECURITY CLASSIFICATION OF THIS PAGE** Unclassified	**19. SECURITY CLASSIFICATION OF ABSTRACT** Unclassified	**20. LIMITATION OF ABSTRACT** UU

NSN 7540-01-280-5500 Standard Form 298 (Rev. 2-89)
Prescribed by ANSI Std. 239-18

THIS PAGE INTENTIONALLY LEFT BLANK

Approved for public release; distribution is unlimited

FRICTION STIR PROCESSING OF AS-CAST AA5083: SUPERPLASTIC RESPONSE

John Toshio Hayashi
Ensign, United States Navy
B.S., United States Naval Academy, 2008

Submitted in partial fulfillment of the
requirements for the degree of

MASTER OF SCIENCE IN MECHANICAL ENGINEERING

from the

NAVAL POSTGRADUATE SCHOOL
June 2009

Author: John Toshio Hayashi

Approved by: Terry R. McNelley
Thesis Advisor

Jianqing Su
Co-Advisor

Sarath Menon
Co-Advisor

Knox T. Millsaps
Chairman, Department of Mechanical and Astronautical Engineering

THIS PAGE INTENTIONALLY LEFT BLANK

ABSTRACT

Plates of continuously cast AA5083 were subjected to friction stir processing (FSP) by three overlapping plunge and traverses. The FSP used a threaded pin tool with a pin diameter of 3 mm, pin length of 3 mm and a shoulder diameter of 10 mm. The process was run at constant tool rotation and traverse speeds of 800 rpm and 76.2 mm min^{-1}, respectively. The microstructure of the processed region was examined by optical microscopy and orientation imaging microscopy. FSP of the AA5083 reduced the average grain size from approximately 60 μm in the base metal to 3-4 μm in the processed zone. In addition, it created a homogeneous microstructure and, in particular, a refined and homogenous particle distribution without damage to the particles. Large tensile samples with gage sections of 1x3x8 mm were prepared by wire EDM for high-temperature tension testing. Tensile tests were carried out at 450°C under different strain rates. The relationship between strain rate and elongation was established. A maximum superplastic elongation of ~550% was obtained at a strain rate of 3×10^{-3} s^{-1}. The formation mechanism of refined grain structure and the superplastic characteristic of FSP material will be discussed in this paper.

THIS PAGE INTENTIONALLY LEFT BLANK

TABLE OF CONTENTS

LIST OF FIGURES

LIST OF TABLES

THIS PAGE INTENTIONALLY LEFT BLANK

ACKNOWLEDGMENTS

I would first like to thank my advisor, Dr. Terry R. McNelley, for all of his guidance throughout this project. Also, I would like to thank Dr. Jianqing Su and Dr. Sarath Menon for donating their time in the laboratory and in the classroom. I am fortunate to have worked with them, and I have learned a great deal. Their teachings have allowed me to accomplish a lot during my short time at the Naval Postgraduate School.

I would also like to thank my family for all of their support throughout my education. Without their love, I would not have been able to accomplish any of the things I have in my life.

My friends have been very instrumental in my education and I would like to take the chance to thank them. Without the study sessions, long nights and group projects I would not have achieved the things that I have.

The Monterey Bay Athletic Club has also played a large role in my development as an officer. I have forged a lifelong addiction to fitness and learned just as much from these classes as any other. Thank you Rachelle, Beth, Nikki, Karen, Dan, Lisa, Audra and Ember for all of the heavy lifting you did.

Go Lightning Strike Pirate Squad!

Finally, cheers to the Baby Nukes for accompanying me on this journey through Monterey and beyond. Best of luck to you all!

THIS PAGE INTENTIONALLY LEFT BLANK

I. INTRODUCTION

The concept of friction stir processing (FSP) is based on a relatively new form of welding developed at The Welding Institute (TWI) in Cambridge, England [1]. Friction stir welding (FSW) uses a rotating tool traversed along the seam of two abutted work pieces to join them together. FSP has the same fundamental concept, but is not a joining process. The tool is plunged and moved in a predetermined pattern to process a volume of material. The tool rotation rate and traverse speed can be modified to change the heat input to the work piece. FSP will promote superplasticity in a material by refining the grain size, homogenizing the particle distribution and increasing the fraction of high angle boundaries.

Superplastic forming is becoming increasingly important due to high demand for lightweight but strong materials. AA5083 is a material of particular superplastic forming interest because of its corrosion resistance, weldability and high strength to weight ratio.

The material investigated in this study is a continuously cast AA5083 in the as-cast condition. The primary goal of this study is to assess the effects of FSP on the material. This will be accomplished by studying the microstructure before and after FSP and testing the mechanical properties of the material, specifically the superplastic behavior.

THIS PAGE INTENTIONALLY LEFT BLANK

II. BACKGROUND INFORMATION

A. ALUMINUM ALLOY 5083

The United States Navy is always considering the most effective and cost effective materials and manufacturing processes. These desires have lead to a long-term interest in aluminum alloys for naval shipbuilding and design. The 5xxx-series aluminum alloys (Al-Mg system) are widely used in many manufacturing applications because of their low cost and beneficial mechanical properties. Specifically, the 5083 alloy is widely used because of its weldability and relatively high strength to weight ratio. Also, the alloy's high corrosion resistance is ideal for exposure to salt water as demanded by the Navy. Currently, the US Navy uses AA5083 in plating and extrusions on several of its ships, including the Littoral Combat Ship and the HSV-1 Swift [2].

In addition to its naval application, AA5083 is also used in the civilian sector of industry. The automotive industry uses the alloy for car chassis, wheels and sub-frames of the vehicle. The weldability of AA5083 makes it an ideal material choice because these components have a high emphasis on welded material strength [3]. Recently, General Motors Corporation has reported on the development of quick plastic forming (QPF) technology for use with AA5083 [4]. QPF involved hot blow forming of AA5083 sheet material to form various automobile body components. This process is similar to superplastic forming (SPF) but takes place at higher strain rates in the range of the transition from grain boundary sliding to dislocation creep whereas SPF is normally done at the low strain rates of the grain boundary sliding regime [5-9]. QPF also takes advantage of the role of the Mg addition to the Al-base alloy, which results in control of deformation by solute drag creep (SDC) in the dislocation deformation regime. The flow stress is more strain-rate sensitive during SDC and this enhances ductility under QPF forming conditions [10-13]. Citing its relatively high strength to weight ratio, Boeing's Commercial Fleet uses AA5083 for parts of the aircraft whose failure would not lead to the total loss of the aircraft. By replacing such parts as older aluminum castings and fiberglass assemblies, Boeing's planes have become lighter, thus making each flight more

cost effective [14]. Through the use of AA5083 the US Navy, along with other commercial industries, are making parts that are lighter, stronger, corrosion resistant, weldable and ultimately cheaper than other materials.

AA5083 can be comprised of various different alloying additions, such as Cu, Mn, Mn+Sc, Sc+Sn, Mn+Zr, Zr and Sc [15]. For this study, a sample of AA5083 with the billet designator, G1, was used. The G1 sample was received in the as-cast condition from Commonwealth Aluminum [16]. Table 1 gives the composition of the G1 sample, which represents a standard 5083 alloy composition.

Table 1. Chemical Composition of G1 Aluminum

Chemical Composition of Alloys	
Element	Weight % for G1
Si	0.102
Fe	0.191
Cu	0.025
Mn	0.735
Mg	4.616
Cr	0.249
Zr	0.001
Al	Balance

B. SUPERPLASTICITY

Superplasticity is a state in which a crystalline material will deform well beyond its normal yield point in tension. As a standard, superplastic behavior occurs at elongations over 200% of the original length [17]. Superplasticity is dependent on the strain rate, as shown in Equation 1 [18].

$$\sigma = K\dot{\varepsilon}^{m} \qquad \text{(Eq.1)}$$

where σ = true stress
$\dot{\varepsilon}$ = natural strain rate
K = constant
m = strain-rate sensitivity index

Most metals will have an m value of around 0.2; superplastic materials often have strain-rate-sensitivity exponents larger than 0.33. Silica glass and polymers, with m=1, are not considered superplastic because they are not crystalline, but rather are referred to as exhibiting Newtonian viscous flow [18].

Superplastic materials have several advantages. With elongations over 200%, and sometimes as large as 1000%, all superplastic materials exhibit excellent deformability. The high ductility allows superplastic materials to be molded into intricate shapes. Continuous cast metals that are not superplastic cannot be used to form small, thin or intricate shapes by plastic deformation because of their low ductility. In these materials, the work-piece ruptures before being formed into the desired shape [19]. The high ductility of superplastic materials also allows them to form large and complex work-pieces in a single operation. The fabrication of large, single-piece structures eliminate the use of joints and rivets that are needed to join other materials. The removal of joints and rivets increases the strength of the work-piece by eliminating sites of potential stress concentrations [20]. Also, by forming only one large work-piece, superplastic materials eliminate the need for extra machining. This also saves money by saving time and does not produce waste or scrap material [20].

Another advantage of super-plastic materials is that they do not have to be heat treated to achieve high ductility. Cast, or continuously cast materials must be heat treated, quenched, and then aged at temperature before being formed into a work-piece. This process is time-consuming and the apparatuses required for this process are expensive. The heat treatment process creates distortions in the CC materials. These distortions must be fixed before final processing can occur, once again slowing down the procedure. Superplastic materials, because they do not need to be heat treated, do not have these residual stresses. The high ductility and ease of processing make superplastic materials an ideal material for many applications.

The microstructure of a material is related to its superplastic behavior. The driving force behind this behavior is a small average grain size. Typical grain sizes are around 20-25 μm in conventional aluminum alloys, but it is understood that a smaller grain size is necessary for superplasticity. The small grain size enables the deformation

of the material by grain boundary sliding, allowing the material to stretch superplastically. Another characteristic of superplastic materials is a large amount of high angle grain boundaries. High angle grain boundaries make it easier for grain boundary sliding to occur, leading to superplasticity. Finally, a homogeneous dispersion of fine-grained particles within the material promotes plastic deformation. Understanding the microstructure of the material leads to an understanding of how to process a material to obtain these characteristics and thus a superplastic material.

There are only a few methods to create superplasticity within a metal. Currently, sheets of continuously rolled AA5083 achieve superplasticity by undergoing cold rolling. The sheet of AA5083 is produced through direct chill casting, and then put through several steps of rolling treatment. Cold rolling is an effective method because it increases the yield strength and hardness of the metal by introducing dislocations into the crystal structure and may reduce the average grain size as well. However, cold rolling is a very costly operation and is only economically viable for large industrial production [15]. In order to overcome these expenses, new methods of creating superplasticity have been developed. Friction stir processing is an emerging technique that can be used to reduce the grain size and thus promote superplastic behavior.

C. FRICTION STIR PROCESSING

The technique of friction stir processing (FSP) is based on a form of welding developed at The Welding Institute (TWI) in Cambridge, England [1]. Friction stir welding (FSW), as developed by TWI, is a solid state joining process that uses a rotating tool to traverse along the seam of two abutted work pieces. FSP is similar in concept, but is not used as a joining process. In FSP, a tool is rotated and plunged into the surface of the work piece. The tool contains a shoulder and a smaller, projecting pin. After the pin has been plunged to the desired depth, the entire tool is traversed along the surface of the work piece in a pre-determined pattern. Figure 1 is a schematic of a single plunge and traverse.

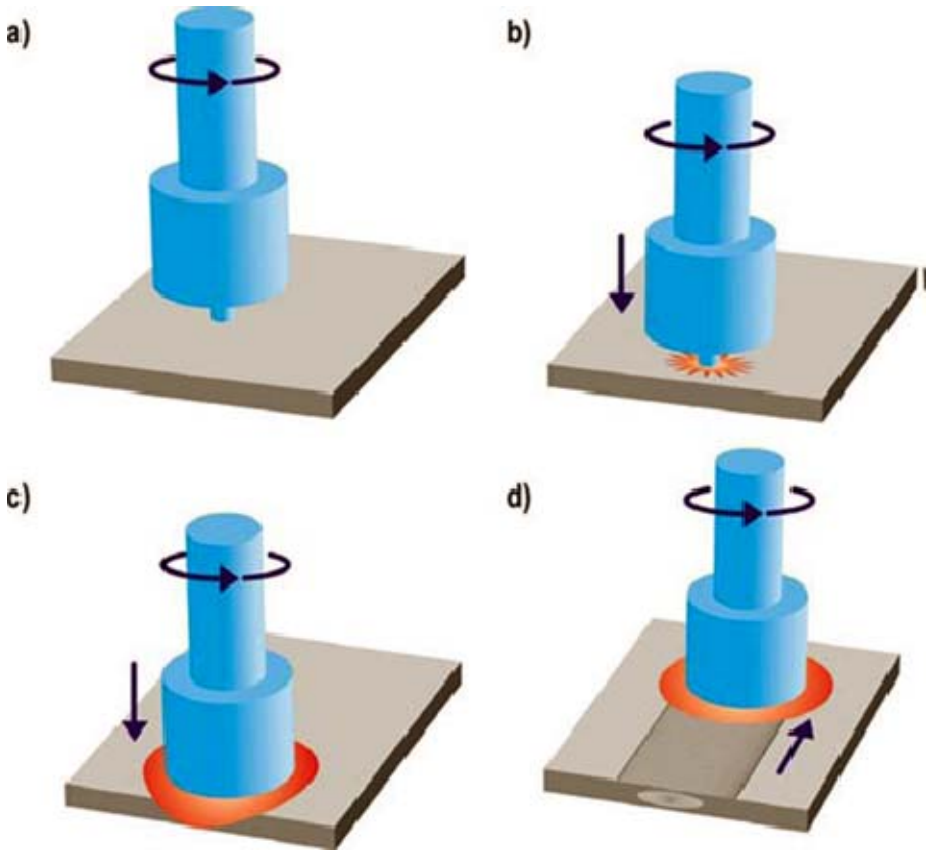

Figure 1. Friction Stir Processing: (a) Rotating Tool (b) Initial Plunge into Surface of Work Piece (c) Plunge to Desired Depth (d) Traverse of Tool. From [21]

The rotation of the tool and the contact with the surface of the work piece creates a large amount of friction. Heat is generated within the work piece, both due to the surface friction and the adiabatic heating from the plastic deformation occurring in the work piece. Due to the heat input, the softened material flows around the pin tool from the advancing side to the retreating side. As the tool continues along its traverse path, the material cools and re-solidifies with a refined grain structure.

It is theoretically stated that a lower heat input during FSP will result in the smaller grain size. Two parameters can be varied in FSP to control the amount of heat input. By slowing the rotation rate of the pin tool, the heat input will be minimized [15]. This assertion is corroborated by the fact that the slower the pin tool rotation, the lower the maximum temperature reached in the processed zone. Another way to reduce the grain size is to increase the traverse rate. Although other factors, such as strain, cooling

rate and tool design play a role in the grain size produced, the general trend of decreasing the tool rotation speed and increasing the traverse rate can be applied to minimizing the grain size. Achieving minimum grain size should maximize superplastic behavior [22].

III. EXPERIMENTAL PROCEDURE

A. OVERVIEW

This research focuses on the microstructure analysis and mechanical properties of friction stir processed AA5083. In order to analyze the changes in microstructure, optical microscopy, as well as scanning electron microscopy (SEM) equipped with orientation imaging microscopy (OIM) was performed. An annealing process was used to measure the effects of extended time at elevated temperature on the grain size in the processed area. Finally, the mechanical properties of the processed AA5083 were assessed using elevated temperature tensile tests. Combining these procedures will provide a method for determining the effectiveness of FSP on creating a superplastic material.

B. FRICTION STIR PROCESSING PROCEDURE

AA5083 samples were received from the manufacturer in the as-cast condition. In order to maximize the amount of material to be processed, the slab of AA5083 was sectioned into 5 mm thick rectangular slabs using wire electrical discharge machine (EDM). Next, the slabs were milled on both sides in order to present a smooth, defect-free surface for friction stir processing. A picture of the AA5083 plate used in FSP is given in Figure 2.

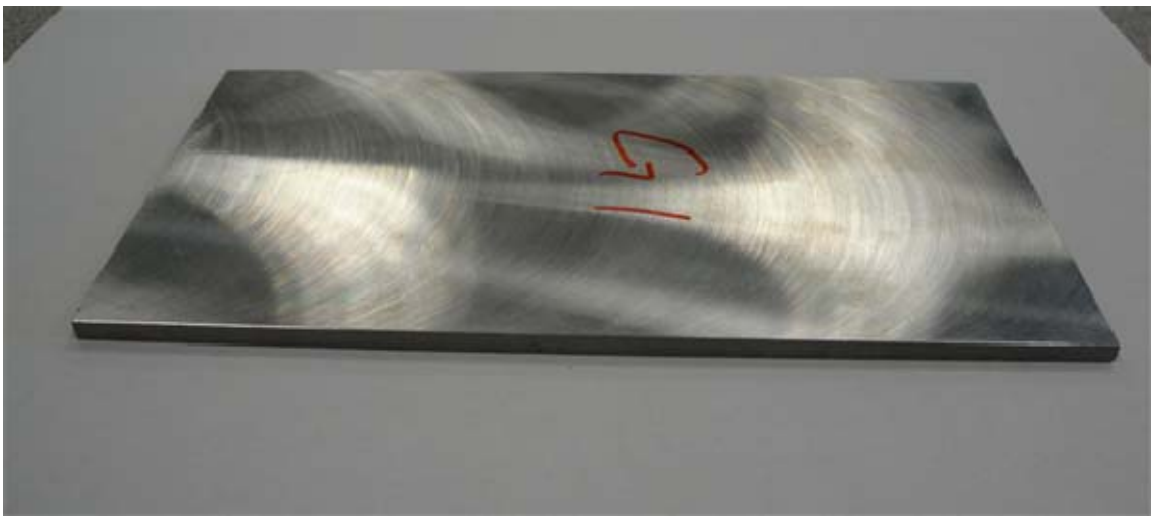

Figure 2. Continuously Cast AA5083 Plate used in FSP

The AA5083 plate was processed using a modified milling machine. The FSP tool was fabricated in H-13 steel and used a threaded pin in order to promote maximum stirring during processing. The pin diameter was 3 mm, the pin length was 3 mm and the shoulder diameter of the tool was 10 mm. A simplified schematic of the tool, showing an unthreaded pin is given in part (a) of Figure 3. Part (b) of Figure 3 gives a schematic of the threaded pin tool design. Figure 4 is a picture of the actual pin tool used in FSP.

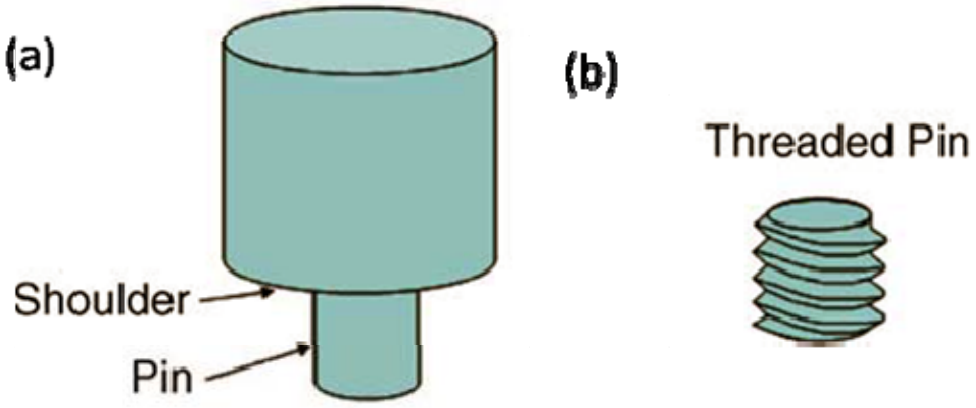

Figure 3. Simplified Tool Design (a) Schematic of Shoulder and Pin (b) Threaded Pin Only. From [22]

Figure 4. Threaded Pin Tool Used in FSP

The plates of continuously cast AA5083 were subjected to FSP by three overlapping plunge and traverses. The process was run at constant tool rotation and traverse speeds of 800 rpm and 76.2 mm min^{-1}, respectfully. A picture of the milling machine used to conduct the processing is shown in Figure 5.

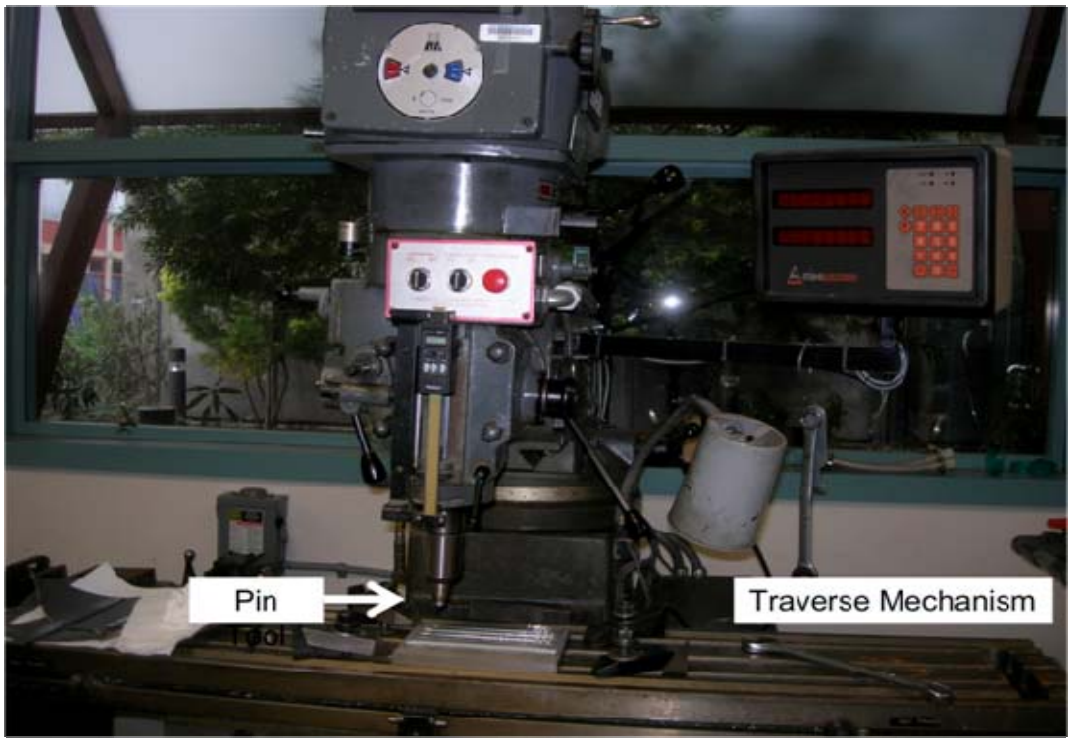

Figure 5. Friction Stir Processing Apparatus

Three overlapping passes were used to create a processed area thick enough to contain the entire tensile sample. One pass was made, and then the pin tool was removed from the surface. The pin was brought back in line with the original entry point before the next pass was made. A step-over distance of 2 mm from the previous pass' centerline was used. The entire pin was plunged into the work piece to a depth where the shoulder enters the work piece. Figure 6 below shows three sets of three plunge and traverses in the aluminum plate.

Figure 6. Continuously Cast AA5083 Plate After FSP

C. MICROSTRUCTURE ANALYSIS OF AS-PROCESSED AA5083

1. Optical Microscopy

a. Sample Preparation

Wire EDM was used to cut a 17 mm x 5 mm x 1.5 mm sample for inspection in the optical microscope. The cut of the sample section was made perpendicular to the transverse axis in order to encompass the processed region and the surrounding base metal. A thermosetting resin was molded around the aluminum sample, exposing only the sample surface. The sample was polished with the Buehler Ecomet 14 Variable Speed Grinder-Polisher in order to eliminate surface defects. Table 2 lists the order of abrasives used to achieve a mirrored finish, free of scratches, on the surface of the specimen.

Table 2. Grinding and Polishing Procedure

Grinding and Polishing Procedure	
Step	Abrasive Used
1	320 Grit SiC Paper
2	600 Grit SiC Paper
3	1200 Grit SiC Paper
4	2400 Grit SiC Paper
5	3 µm Metadi Diamond Suspension
6	1 µm Metadi Diamond Suspension
7	0.5 µm Metadi Diamond Suspension

After polishing, the samples were etched to highlight the large amounts of energy stored along the grain boundaries. The etching solution is comprised of 10% phosphoric acid (H_3PO_4) and 90% water. The solution was heated to 50ºC, and then the sample was immersed in the heated liquid for three minutes. Once etched, the sample was removed and rinsed with ethanol to remove the excess solution from the surface. Finally, the sample was dried using a heat gun to prevent the formation of water spots.

b. Optical Microscopy Procedure

A Nikon Ephiphot 200 optical microscope was used to observe the microstructure of the etched samples. Pictures were taken at low magnification before transitioning to higher magnification to allow for more detail. Sections of the entire surface were captured at low magnification and arranged to create a montage of the entire stir zone. The microstructures of different regions of the sample were studied by optical microscopy. While the depth was tried to be kept constant, two sites were changed to see the variation in microstructure from the top to the bottom of the stir zone. These micrographs extend from the base metal through a heat-affected zone (HAZ), a thermo-mechanically affected zone (TMAZ) and into the stir zone.

2. Scanning Electron Microscope (SEM)

a. Sample Preparation

Two mm thick SEM samples were cut from the middle of the FS processed zone. The cut of the sample section was made perpendicular to the transverse axis in order to encompass the entire stir zone. Each of the samples was polished as if being prepared for optical microscopy. However, in addition to the grinding wheels, each sample was polished using the Electromet4 Electropolisher power supply and cell module. The polishing solution was 80% ethanol, 6% perchloric acid and 14% water. Each sample was electro-polished for 20 seconds using a voltage of 15 volts. Once the sample had been electro-polished, it was placed in the SEM for inspection using orientation imaging microscopy.

b. Orientation Imaging Microscopy Procedure

Orientation imaging microscopy was performed by the TOPCON SM510 scanning electron microscope. Two sets of scans were performed on the as processed AA5083 sample with a scan step of 0.5 μm. The first set was comprised of two different areas: the base metal and the stir zone. The second set contained scans from the top, middle and bottom, but all within the stir zone. Once each of the scans had been performed, the data was analyzed using the orientation imaging microscopy (OIM)

software. In order to create a clean image, software cleanup tools were used. The first setting was grain dilation with a grain tolerance angle of five and a minimum grain size of two points. Next was the grain confidence index standardization, which used the same settings as the grain dilation and tolerance angle. Finally, the neighbor confidence index was set to 0.05. The OIM software provided both numerical and graphical data outputs.

D. ANNEALING OF FSP AA5083

In order to simulate the time spent at elevated temperature during tensile testing, samples of FS processed aluminum were placed in an oven set to 450ºC. A K-type thermocouple was used to ensure that the temperature at the sample location was 450ºC. Five samples were cut from the FS processed zone and had the same dimensions as those used for optical microscopy. Each sample was left in the furnace for a different amount of time. Table 3 gives the times each sample spent at the elevated temperature. Once the samples had been removed from the furnace, they were air cooled to room temperature.

Table 3. Annealing Times

Sample	Time (min)
1	30
2	45
3	60
4	120
5	240

E. MICROSTRUCTURE ANALYSIS OF ANNEALED SAMPLES

1. Optical Microscopy

The optical microscopy procedure was the same as the as-processed condition. However, instead of creating a montage, single micrographs were obtained for each temperature. Micrographs were taken in the base metal, at the stir zone boundary and in the middle of the stir zone.

2. Scanning Electron Microscopy (SEM)

The microstructure of the sample annealed for 240 minutes was studied using OIM and SEM. OIM data was collected from at TSL OIM system equipped in the TOPCON SM510 SEM. A scan of the sample annealed for 240 minutes was completed and cleaned up using the same parameters as before. The backscatter images of the base metal and stir zone were obtained from the Zeiss Neon SEM. Figure 7 shows a picture of the Zeiss Neon SEM.

Figure 7. Zeiss Neon Scanning Electron Microscope

F. MECHANICAL TESTING

1. Tensile Sample Design

Large tensile samples were created to test the superplasticity of the FS processed AA5083. With a limited amount of material, tensile samples needed to be designed carefully in order to maximize the number of samples, but also maintain size integrity. The design dimensions used for the tensile sample are given in Figure 8 below.

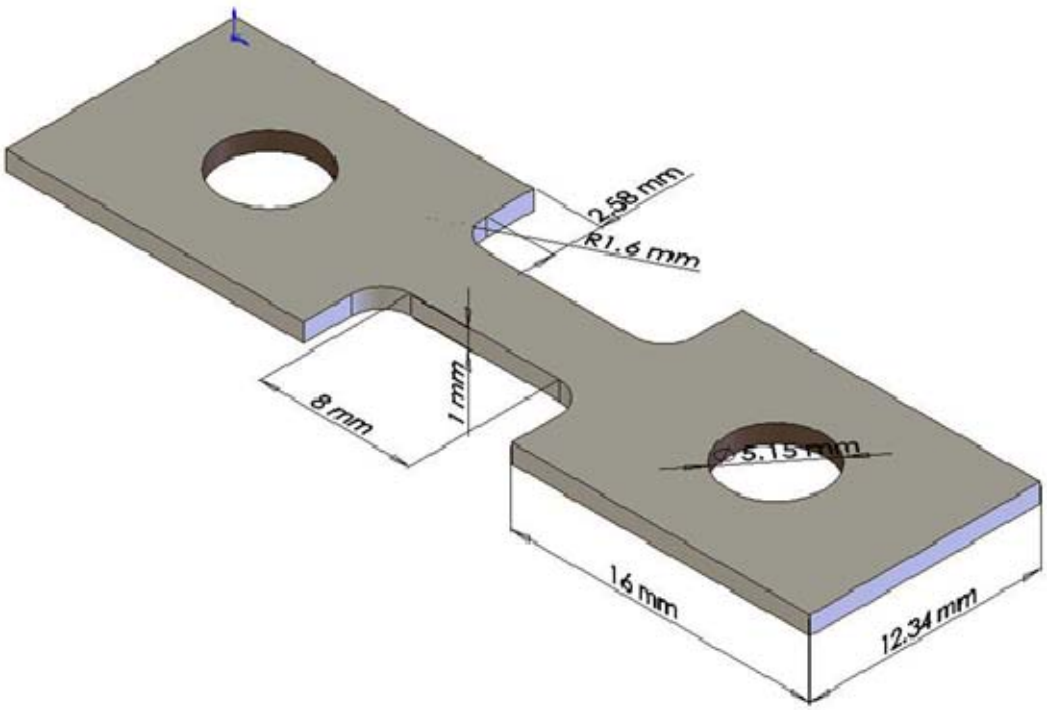

Figure 8. Tensile Sample Dimensions. From [16]

2. Tensile Sample Fabrication

The tensile samples were cut using wire EDM and a program, which defines the dimensions of the tensile sample. The initial starting point and origin for the program was selected to ensure that the gage section of the tensile sample was in the middle of the three traverses.

Once the tensile samples had been cut, each needed to be prepared for use in the Instron tensile testing machine. In order for the grips to be clamped to sample, holes must be drilled into the tensile sample. A #13 drill bit was used to create the hole. Next, the samples were polished using the same abrasives and procedure as if being prepared for optical microscopy. Finally, the side of the gage section was polished by hand using 600 and 1200 grit SiC paper.

3. Superplastic Testing

In order to test the superplastic behavior of the FS processed AA5083, tensile samples were pulled to failure at elevated temperature. The furnace attached to the Instron testing machine was heated to 450ºC and allowed to remain at temperature for one hour. Figure 9 shows the entire Instron apparatus with the furnace doors closed.

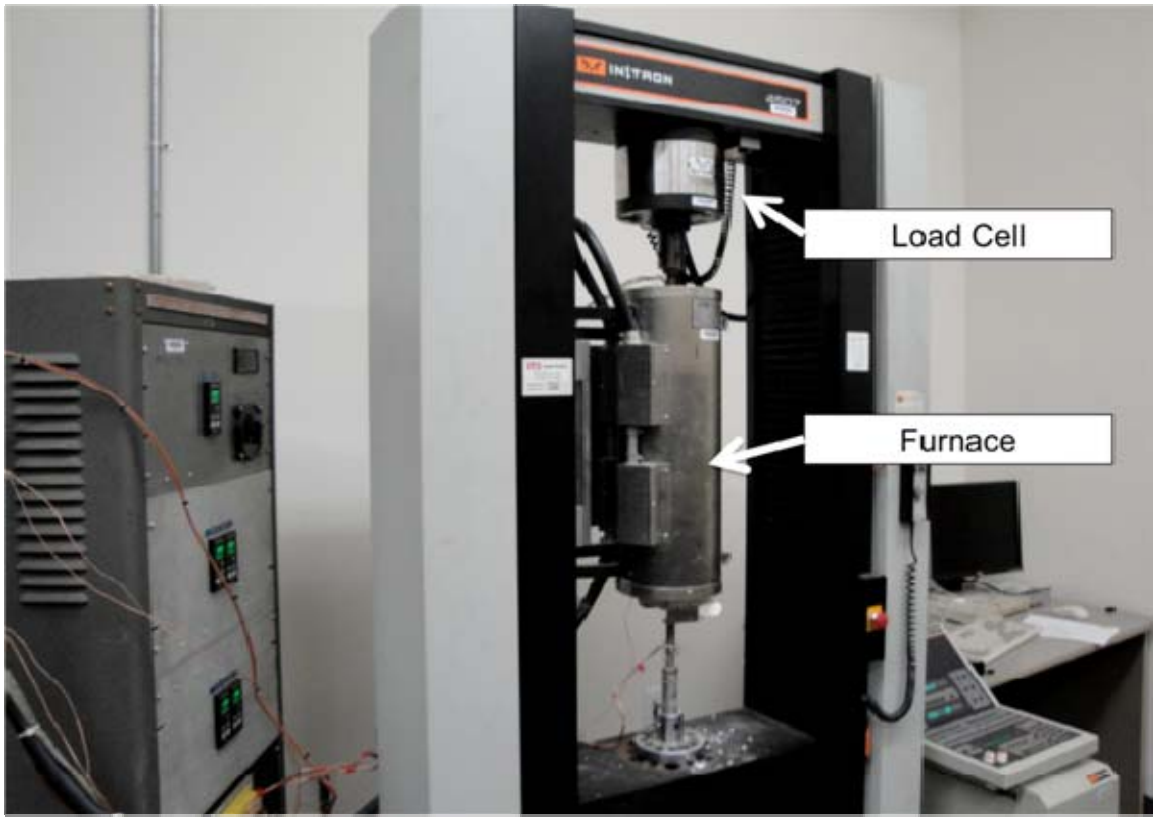

Figure 9. Instron Tensile Testing Machine with Furnace

Outside of the furnace, a tensile sample was clamped in the grips, with special attention paid to ensuring that the gage section of the specimen was not bent. Once the temperature in the furnace reached 450ºC, the sample was placed in the grips and allowed to equilibrate at temperature for 45 minutes. The sample was placed in the second of five regions of the furnace. This ensured that as the sample was elongated downward, the gage section would remain in the middle of the furnace. Figure 10 shows the grips of the Instron machine where the sample was inserted. Once the sample had reached 450ºC, the Instron program was run and the sample was pulled to failure at a constant rate.

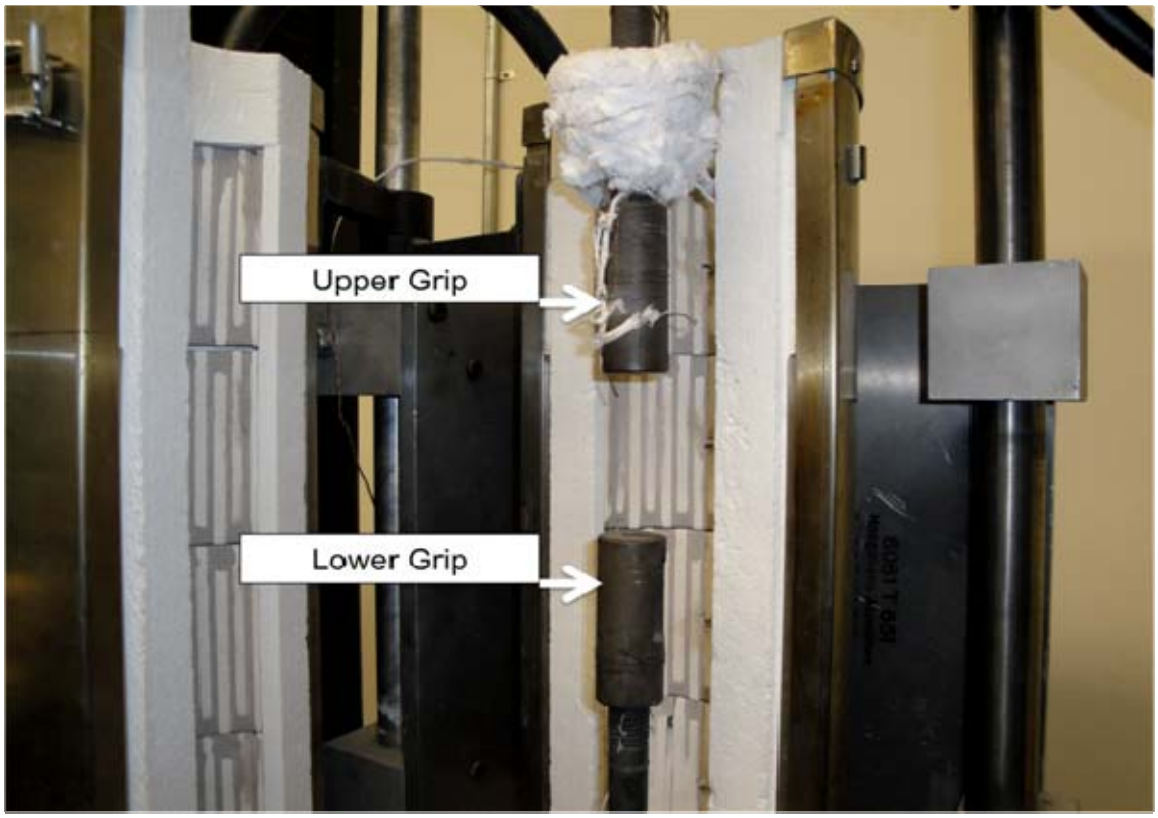

Figure 10. Instron Machine Sample Grips

Table 4 gives the strain rates tested. The corresponding rate in mm/min was based on a nominal gage length of 8 mm. This rate was used in the Instron program to control the rate at which the grips moved apart.

Table 4. Strain Rates

Strain Rates		
Test	Strain Rate (s^{-1})	Strain Rate (mm/min)
1	3×10^{-4}	0.144
2	1×10^{-3}	0.48
3	3×10^{-3}	1.44
4	1×10^{-2}	4.8
5	1×10^{-2}	4.8
6	3×10^{-2}	14.4
7	1×10^{-1}	48.0
8	1×10^{-1}	48.0
9	3×10^{-1}	144.0

THIS PAGE INTENTIONALLY LEFT BLANK

IV. RESULTS

A. OVERVIEW

The results obtained from each of the studies will be presented in this section. The microstructure analysis will be based on the optical micrographs, orientation imaging microscopy results and the backscattered electron images. Finally, the results from the elevated temperature tensile tests will be discussed.

B. MICROSTRUCTURE ANALYSIS OF AS-PROCESSED AA5083

1. Optical Microscopy

Figure 11 shows a montage at low magnification of a cross-section of the as-processed sample in a plane perpendicular to the tool traverse direction.

Figure 11. Low magnification montage of as-processed AA5083 showing a stir zone created by FSP at tool rotation speed of 800 rpm and traverse rate of 76.2 mm min^{-1}. The stir zone is identified by the grain refinement and flow pattern. The numbers show the sites of optical micrographs.

The stir zone is distinct from the base metal and shows a refined grain structure. In addition, a flow pattern is visible within the stir zone. These “onion rings” are the result of the tool traversing and rotating at the same time. The stir zone is intact and does not contain a tunneling defect found in previous work. Figure 12 compares two stir zones: a defect free stir zone created in this study and a stir zone with a tunnel defect.

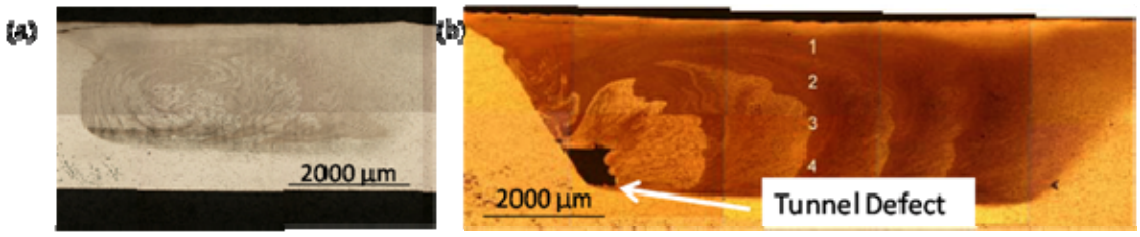

Figure 12. (a) Intact stir zone apparently free of macroscopic defects created by FSP at 800 rpm, 76.2 mm min^{-1} and a threaded pin. (b) Tunnel defect in lower corner of stir zone, created by FSP at 350 rpm, 101.6 mm min^{-1} and a smooth pin. Material processed for Bland thesis work completed in 2006. From [16].

The tunnel defect was formed in a plate processed by a smooth pin at a tool rotation rate of 350 rpm and traversing rate of 101.6 mm min^{-1}. A combination of the threaded pin design and processing parameters has contributed to the elimination of this defect.

Higher magnification pictures were taken at various points across the surface of the FS processed sample. Figure 13 provides the optical micrographs from the seven numbered locations given in Figure 11. Sites 4 and 5 are not in line with the other sites in order to show the variation in grain structure with depth.

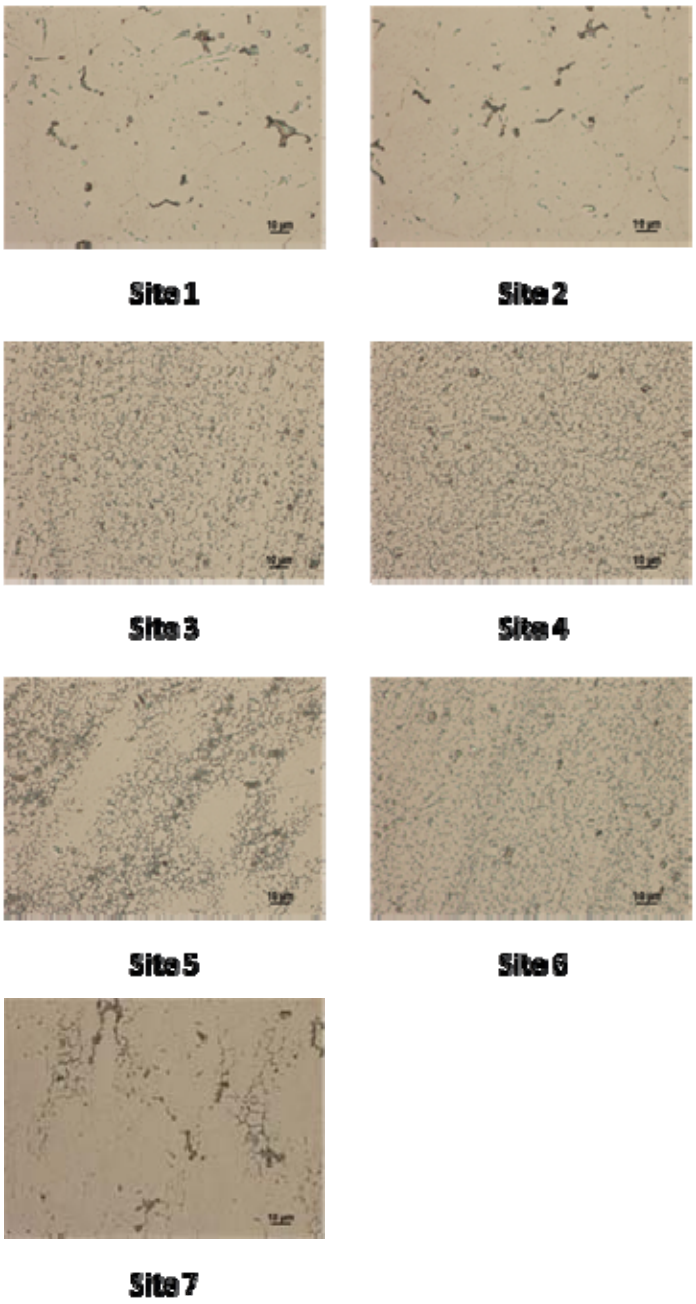

Figure 13. Optical micrographs taken from the as-processed AA5083 sample. Pictures start in the base metal, extend through the heat affected zone (HAZ), the thermo-mechanically affected zone (TMAZ) and into the stir zone. Site 7 is in the HAZ on the far side of the stir zone. The stir zone is identified by a refined grain structure and a homogeneous particle distribution.

Sites 1 and 2 are in the base metal. Sites 3, 4, 5, and 6 are within the stir zone, with site 5 being towards the bottom of the stir zone. Site 7 is in the HAZ on the far side of the stir zone. The base metal can be identified by a larger grain structure and non-uniform dispersion of constituent particles. The higher magnification micrographs taken within the stir zone reveal a refined grain structure. In addition, the particle distribution has become more homogeneous throughout. Site 5 is towards the bottom of the stir zone and close to the interface, and can be identified as such because the plastic deformation flow pattern produces a striping pattern. Site 7 can be identified as in the HAZ, and has a similar grain structure as the base metal. Overall, the low magnification optical micrographs show a distinct stir zone created by FSP. The high magnification micrographs reveal a refined grain structure as well as a homogeneous dispersion of particles within the stir zone.

2. Scanning Electron Microscope (SEM)

The grain sizes in the stir zone created by FSP were too small to be clearly resolved by optical microscopy. In order to measure the grain size, orientation imaging microscopy (OIM) was carried out in the SEM. The first set of OIM scans compared the base metal and the stir zone. The scan measured an 800 μm x 1000 μm area of the sample surface. The surface scanned is transverse to the direction of tool advance and is shown in Figure 14. Figure 15 and 16 show the grain distribution, grain misorientation angle and (001) pole figures for the base metal and stir zone, respectively. Figure 17 provides a comparison of the average grain size between these two regions. The SEM software may be used to determine the average area of each grain. This value is converted to a circle of equivalent area and the equivalent diameter is then calculated.

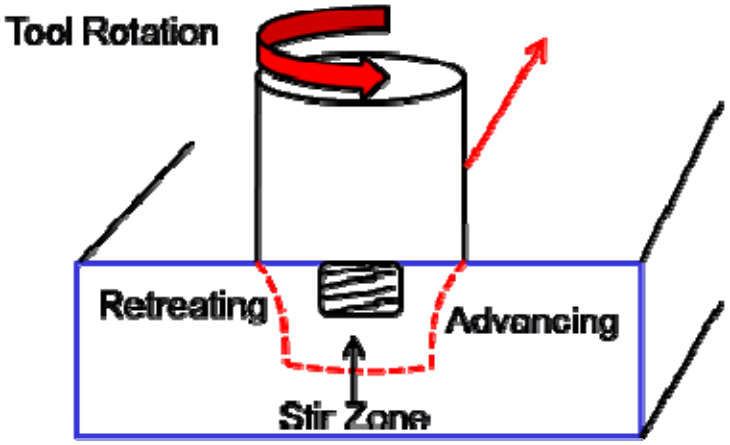

Figure 14. Schematic of the friction stir process. The pin is plunged into the surface, creating a stir zone within the volume of material. The advancing side is shown on the right of the pin tool and the retreating side is shown on the left. The face used for optical microscopy as well as the OIM scans is outlined in blue.

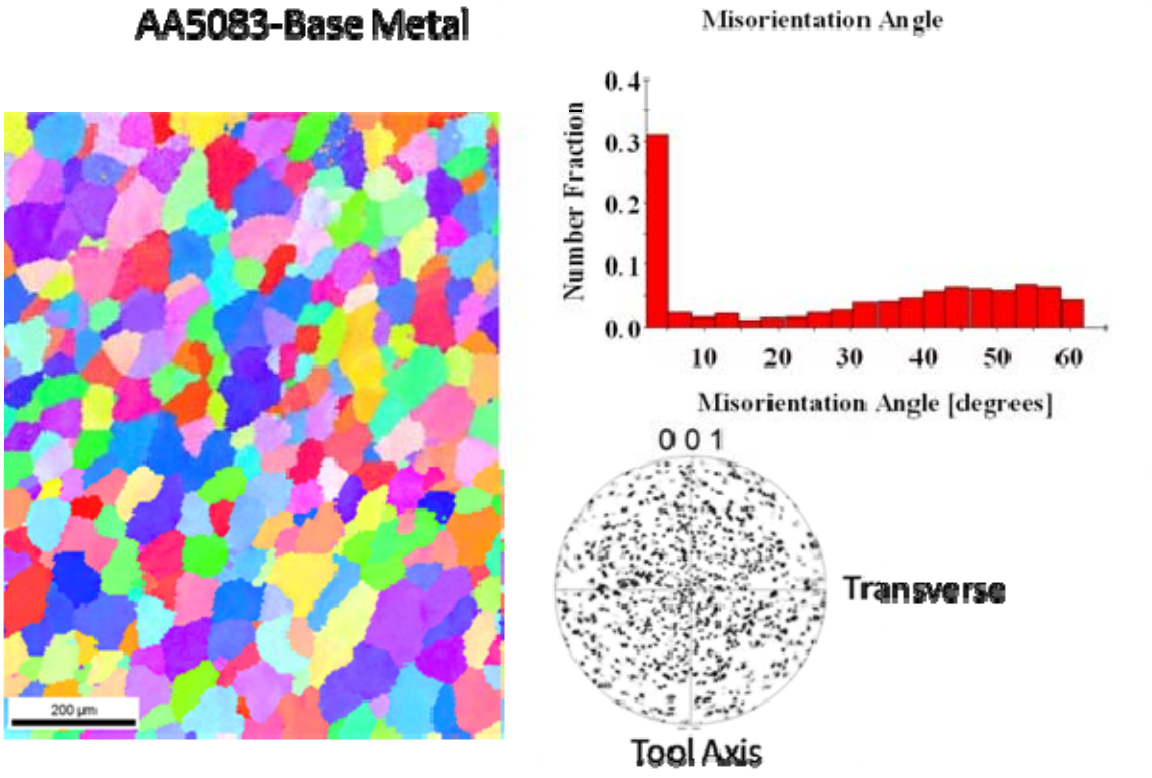

Figure 15. OIM Results for Base Metal: Results show a large average grain size of 70 µm. There are 65% high angle grain boundaries. The large fraction of low angle boundaries is presumably the result of the rolling operation during continuous casting. The (001) pole figure reveals a random texture.

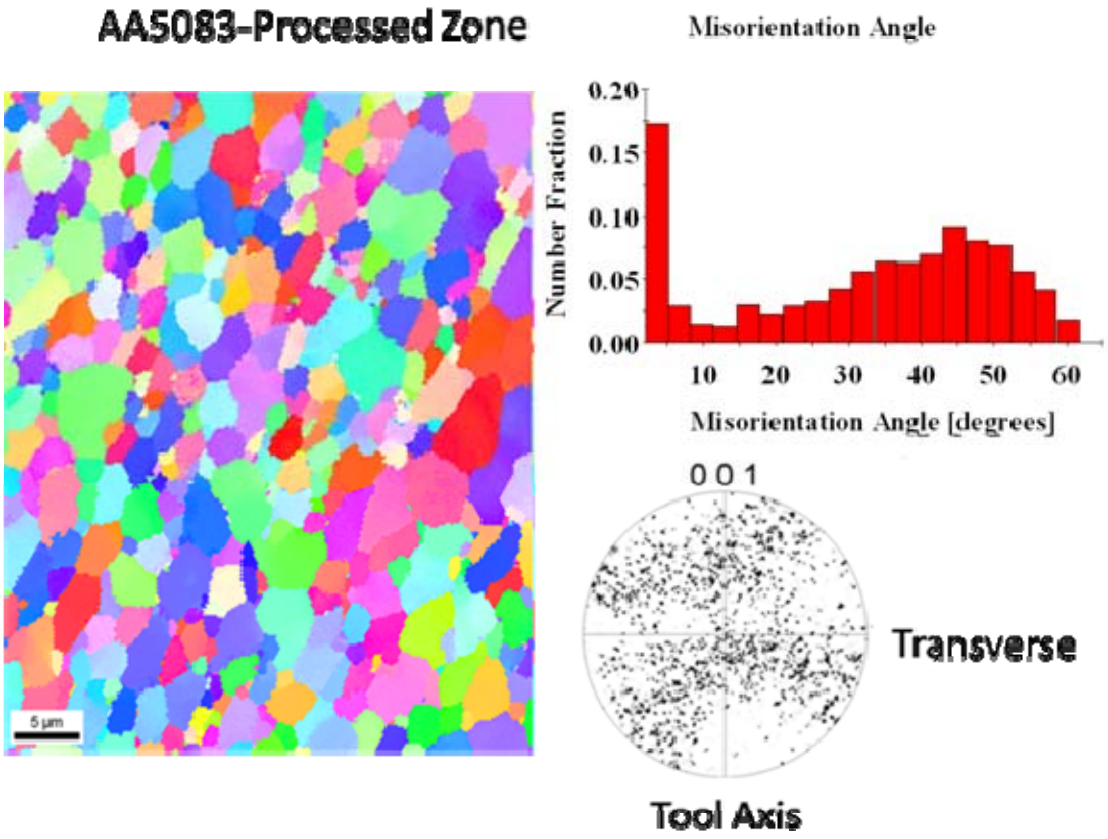

Figure 16. OIM Results for Processed Zone: Results reveal a refined, equiaxed grain structure with an average grain size of 4 µm. The fraction of high angle grain boundaries has been increased to 80%. The reduction of low angle boundaries suggests that FSP allows the sample to approach compete recovery and recrystallization. The (001) pole figure reveals a weak deformation texture.

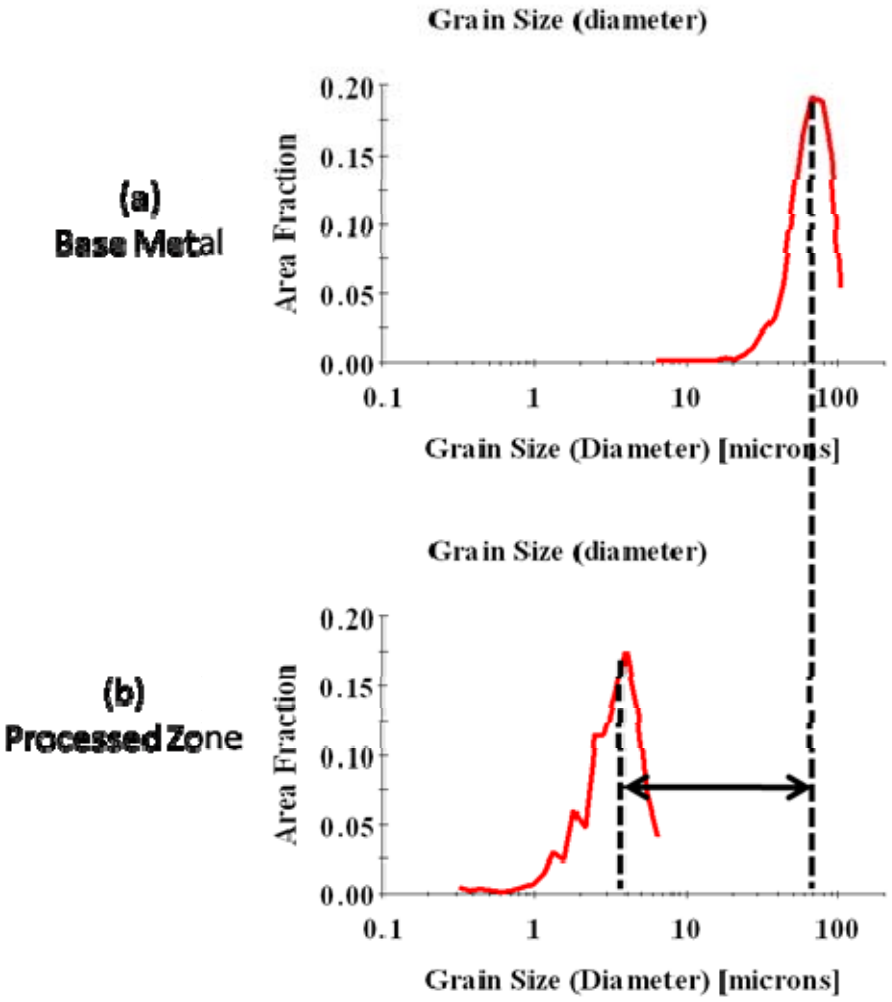

Figure 17. Comparison of grain size between (a) base metal and (b) processed zone of FSP AA5083. The average grain size in the base metal is 70 μm while the average grain size in the processed zone has been reduced to 4 μm.

As shown in Figure 15, the base metal has a large grain size, high fraction of low angle boundaries and a random texture. Figure 16 shows that substantial changes have been made to the microstructure in the stir zone. In the base metal, 65% of the boundary angles are high angle boundaries (>15º). This value has been increased to 80% within the processed zone. FSP has also added a weak deformation texture to the processed zone while the texture of the base metal appears to be random. The grain structure of Figure 16 and the graphs of Figure 17 reveal that the grains in the processed zone are significantly smaller than in the base metal. The average grain size in the base metal is ~70 μm. This has been reduced to ~4 μm inside of the stir zone.

Three more OIM scans were performed inside the stir zone to examine the variation in grain size with depth. Figure 18 shows the location depths of the scans made as well as the OIM results depicting grain structure, texture and grain size.

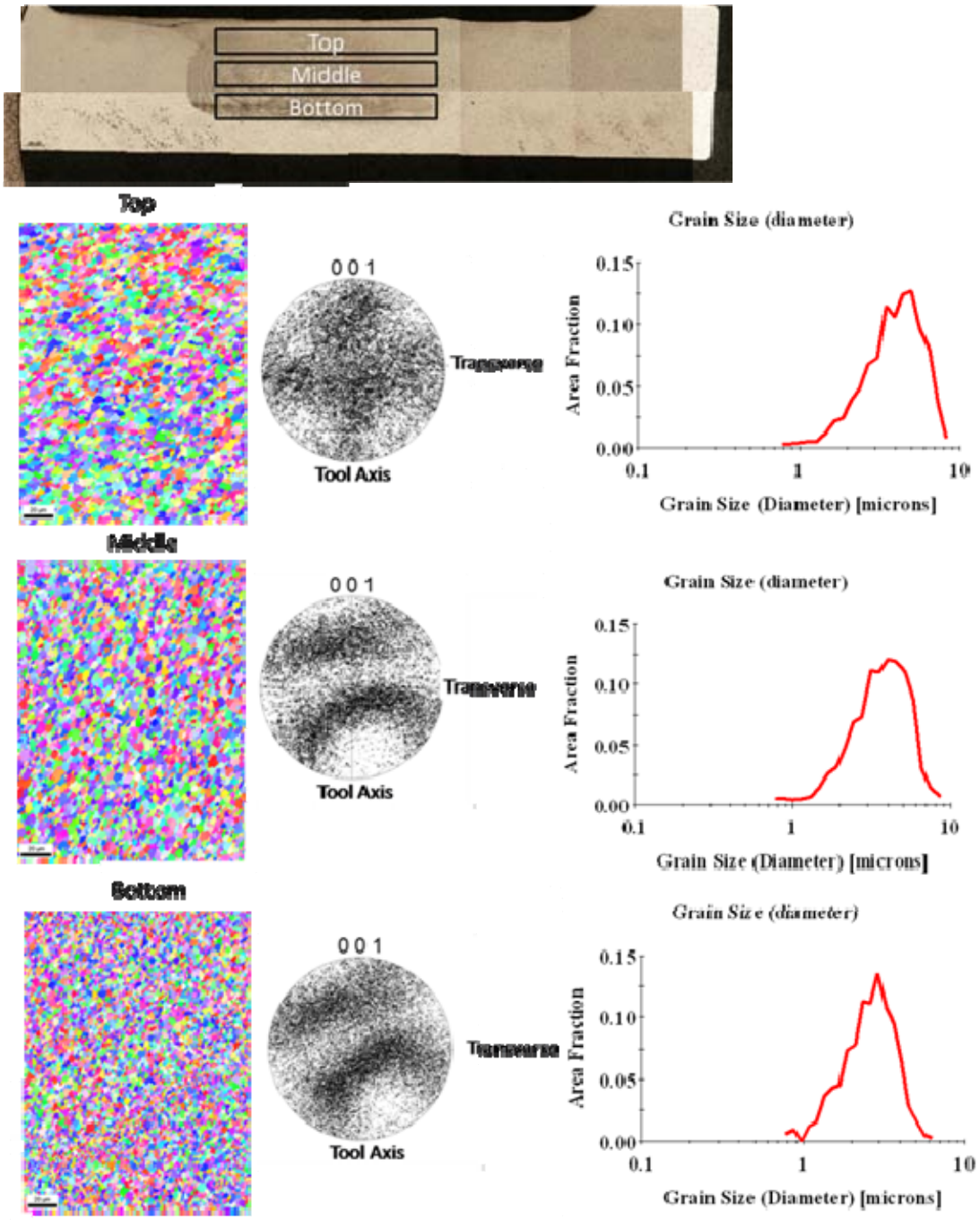

Figure 18. Low magnification micrograph of stir zone depicting three locations within the stir zone where OIM scans were performed. OIM scans reveal a uniform microstructure and the presence of a weak deformation texture. The grain size is fairly uniform: 5 μm in the top, 4 μm in the middle and 3 μm in the bottom.

The grain structure is similar for each region, and shows a refined size and equiaxed structure. All three areas contain a similar texture. The grain size has been refined, with the most refinement coming at the bottom of the stir zone. From top to bottom, the grain size slightly decreases, from 5 μm at the top to 4 μm in the middle to 3 μm in the bottom. These scans show that a basically uniform microstructure has been achieved throughout the stir zone. From the OIM scans, it can be concluded that FSP created a uniformly refined, equiaxed grain structure, increased the fraction of high angle grain boundaries. Refinement of particle size and a more homogeneous distribution of the precipitate phase also accompanied the grain refinement during FSP.

C. MICROSTRUCTURE ANALYSIS OF ANNEALED AA5083

1. Optical Microscopy

The annealed samples were examined under the optical microscope. Figure 19 provides micrographs in the base metal and processed zone for each annealing time.

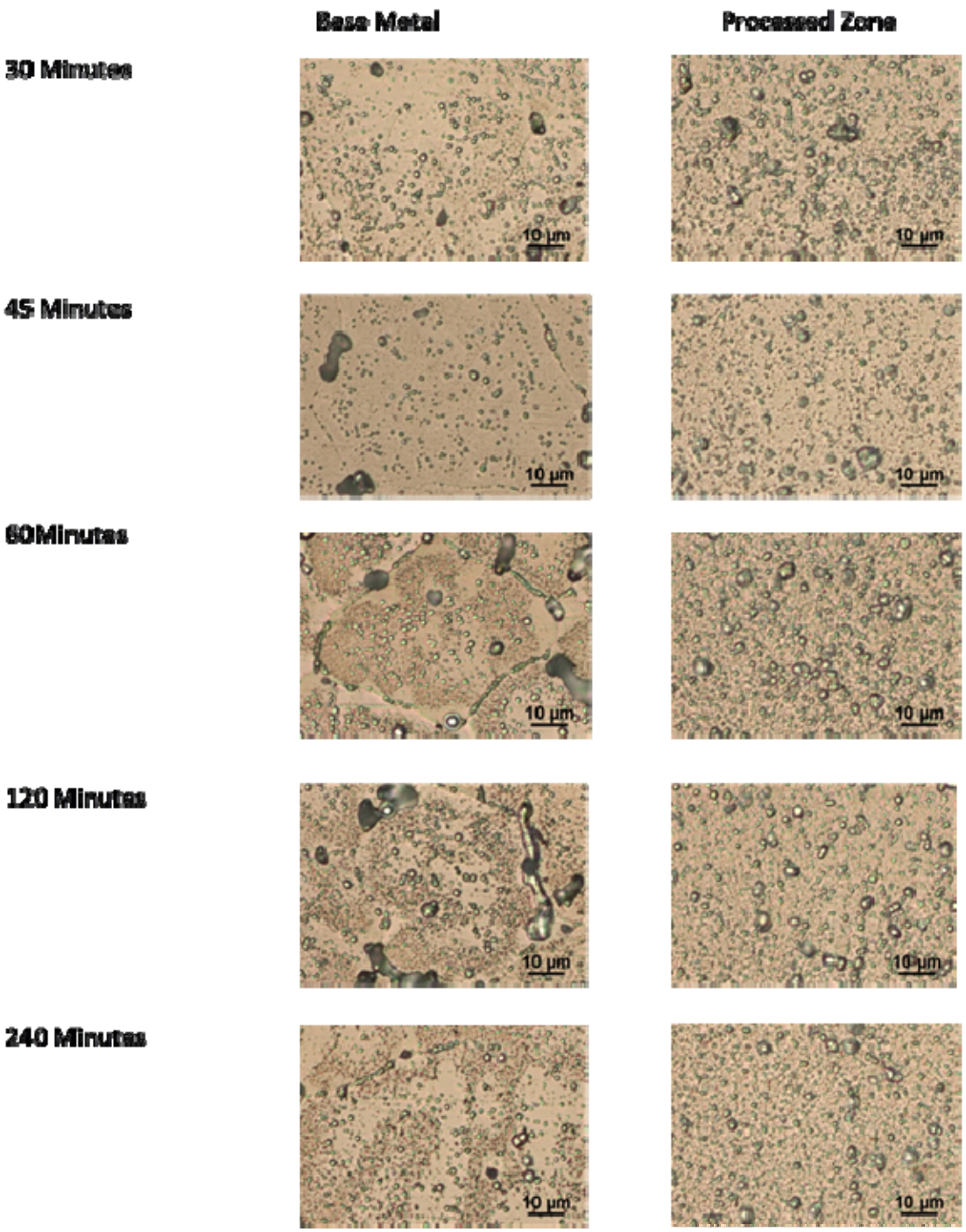

Figure 19. Optical micrographs in the base metal and processed zone of FS processed AA5083 samples annealed at 450ºC. The micrographs reveal stable grain growth in both regions. There was no evidence of any abnormal grain growth in these samples. Some studies have reported abnormal grain growth in AA5083 during FSP or after subsequent heat-treatment at high temperature [5].

Due to a very small grain size, the grain boundaries, and thus the average grain size, cannot be identified on the micrograph. However, it is possible to discern that no abnormal grain growth has occurred, which would cause the grains to grow exponentially with time. In order to determine the grain size, OIM was performed. The precipitate distribution in these samples was quite uniform even after annealing and unlike the base material, large precipitates were not observed along the grain boundaries.

2. Scanning Electron Microscope

a. OIM

OIM was used to analyze the microstructure of the sample annealed for 240 minutes. Figure 20 shows the grain distribution, grain boundary misorientation angle and the (001) pole figure for the annealed sample.

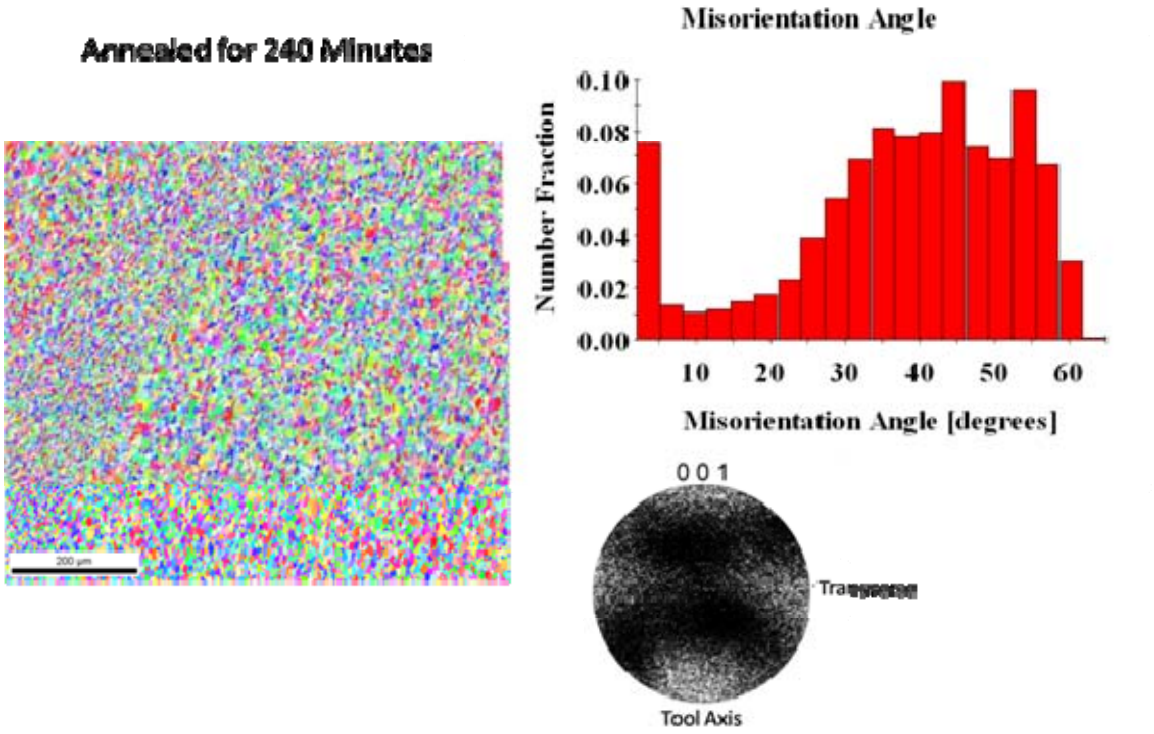

Figure 20. OIM results for a FS processed AA5083 sample annealed at 450ºC for 240 minutes. These images showed a refined grain structure in general, but often banded regions with slightly larger grains were observed. The fraction of high angle grain boundaries is 90%. The (001) pole plot reveals a slight deformation texture consistent with the as-processed sample.

Following the prolonged annealing at elevated temperature, 90% of the grain boundaries were high angle boundaries. Also, the deformation texture pattern was retained. From the grain distribution plot, it can be seen that the microstructure is still refined. The grains in the annealed sample remain equiaxed but there were regions (or bands) where the grains were somewhat larger. Figure 21 provides a comparison of the as-processed AA5083 and a sample that had been annealed for 240 minutes.

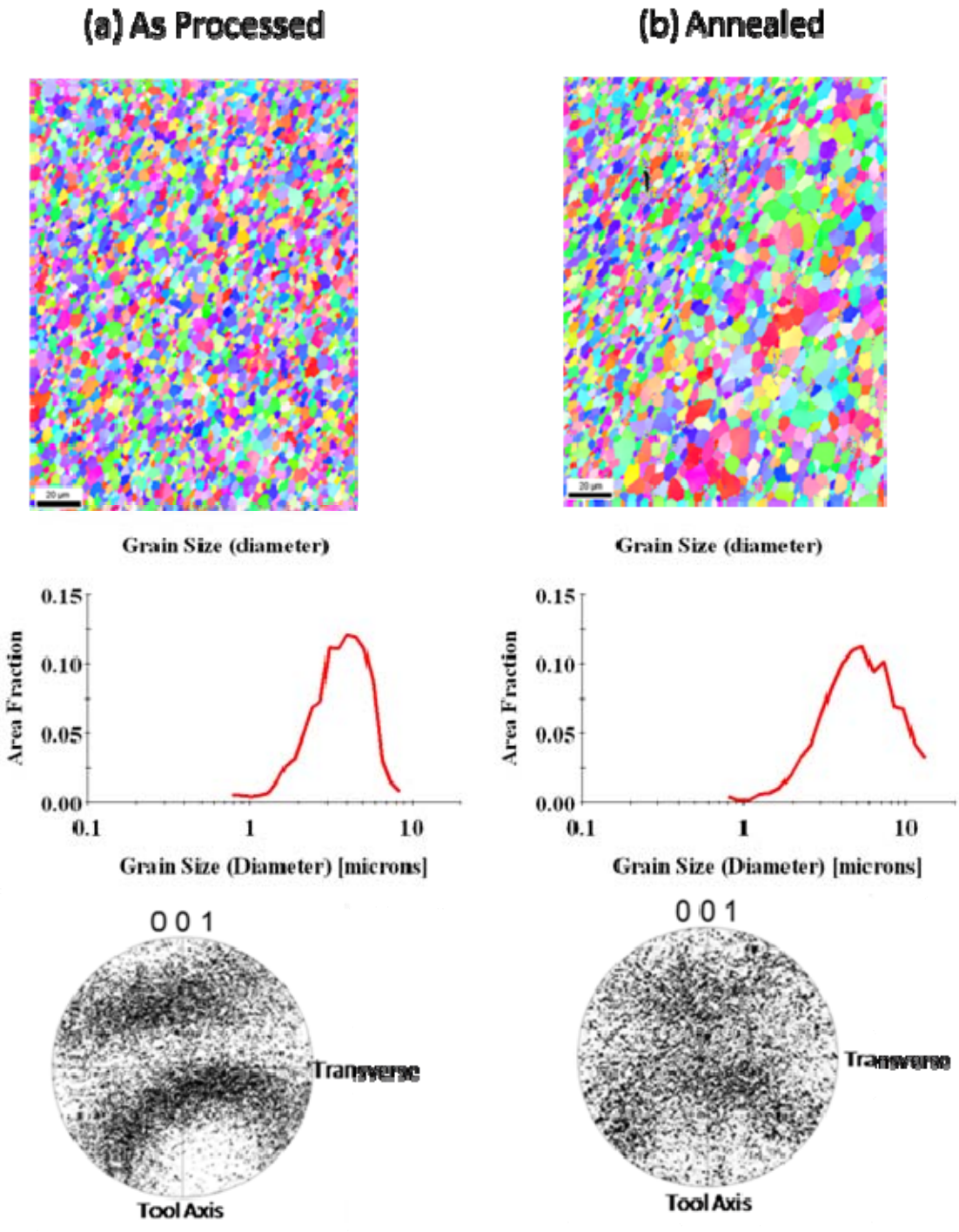

Figure 21. Microstructure comparison of FS processed AA5083 in the (a) As-processed condition and (b) after annealing at 450ºC for 240 minutes. OIM results show that the grain structure is still refined and equiaxed, and the average grain size has grown from 4 µm to 5 µm. It appears that the deformation texture is retained in the samples even after a prolonged aging at 450ºC.

These results show that annealing the friction stir processed AA5083 results in very restricted grain growth even after 240 minutes exposure at 450ºC. The deformation texture produced during the tool rotation appears to be retained even after long term annealing at high temperature. The average grain size in the as-processed material was 4 µm. After 240 minutes, the average grain size had grown to 5 µm.

b. Back-Scattered Electron (BSE) Imaging

BSE images, as well as in-lens secondary electron (SE) images were obtained using the Zeiss Neon SEM and are presented in Figure 22. These images show the grain structure of the FS processed AA5083 in both the as-processed and annealed condition. Figure 22a shows a low magnification BSE image representing both the processed zone and the base metal. The processed zone is at the top of the frame and is characterized by the fine microstructure. The base metal is in the bottom of the frame and an interface region between the two is identified by an elongation of the grains. Figure 22b and Figure 22c are in-lens SE images showing high magnification pictures of the grain structure within the processed region. The grains are equiaxed and the average grain size appears to be 1 µm. Figure 22d is a BSE image of the sample that had been annealed for 240 minutes at 450ºC. The micrograph shows coarsened grains with a grain size of approximately 5 µm. The presence of precipitates (appearing white) is also visible on the image. The precipitates are homogeneously distributed throughout the area and are presumably the Al_6Mn phase.

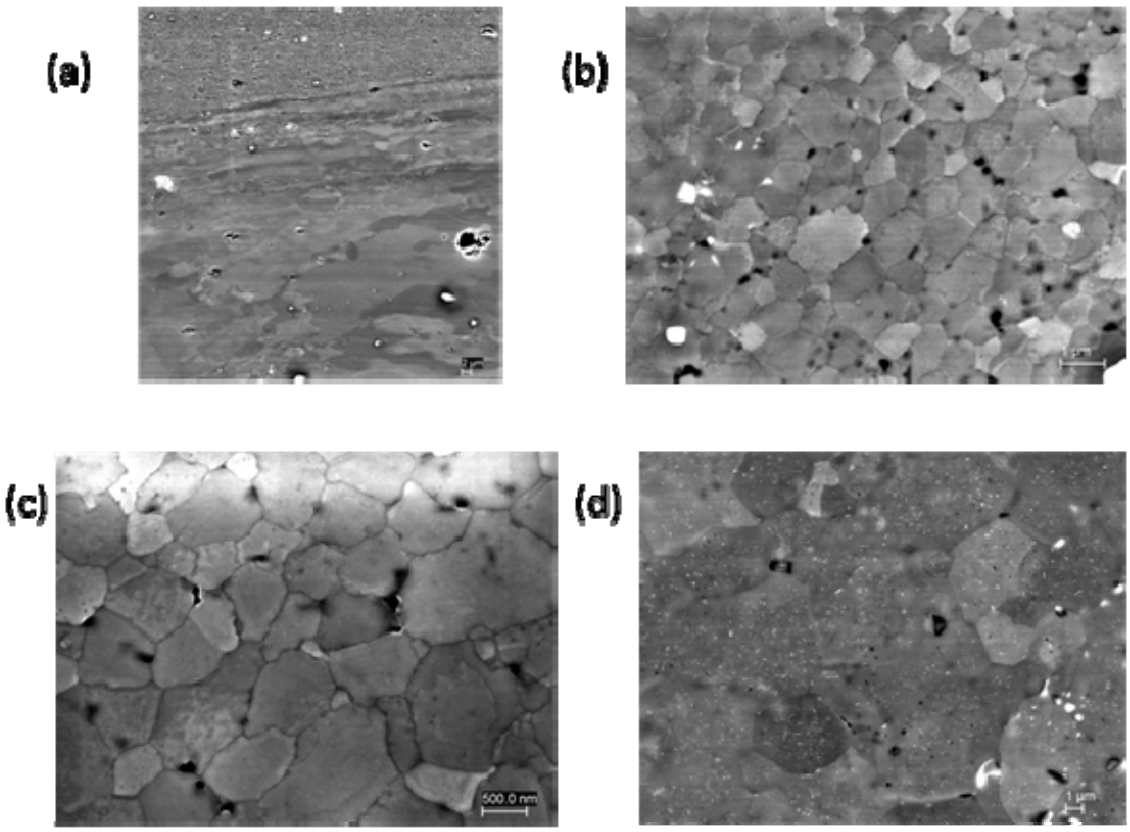

Figure 22. BSE and SE images obtained for FS processed AA5083 (a) As-processed condition showing refined grain structure in processed zone and elongation of grains in the base metal. (b) Processed region showing equiaxed grain structure (c) Processed zone at high magnification showing an average grain size of 1 µm. (d) Annealed sample at 450ºC for 240 minutes showing equiaxed grains in the processed region with an average grain size of 5 µm. Homogeneous distribution of particles is also visible.

D. MECHANICAL TESTING

Nine samples were pulled to failure at elevated temperature using different strain rates. Table 5 gives the elongations for each strain rate. The elongation percentages were based on an original gage length of 8 mm. Figure 23 shows a photograph of all the tested samples, arranged from lowest strain rate at the top to the largest strain rate at the bottom.

Table 5. Results from tensile tests of FS processed AA5083 samples at 450ºC. A maximum elongation of 633% occurred at a strain rate of 1×10^{-2} s^{-1}. The elongation percentages were based on a starting gage length of 8 mm.

Superplastic Testing		
1	3×10^{-4}	243%
2	1×10^{-3}	380%
3	3×10^{-3}	550%
4	1×10^{-2}	430%
5	1×10^{-2}	633%
6	3×10^{-2}	500%
7	1×10^{-1}	160%
8	1×10^{-1}	143%
9	3×10^{-1}	100%

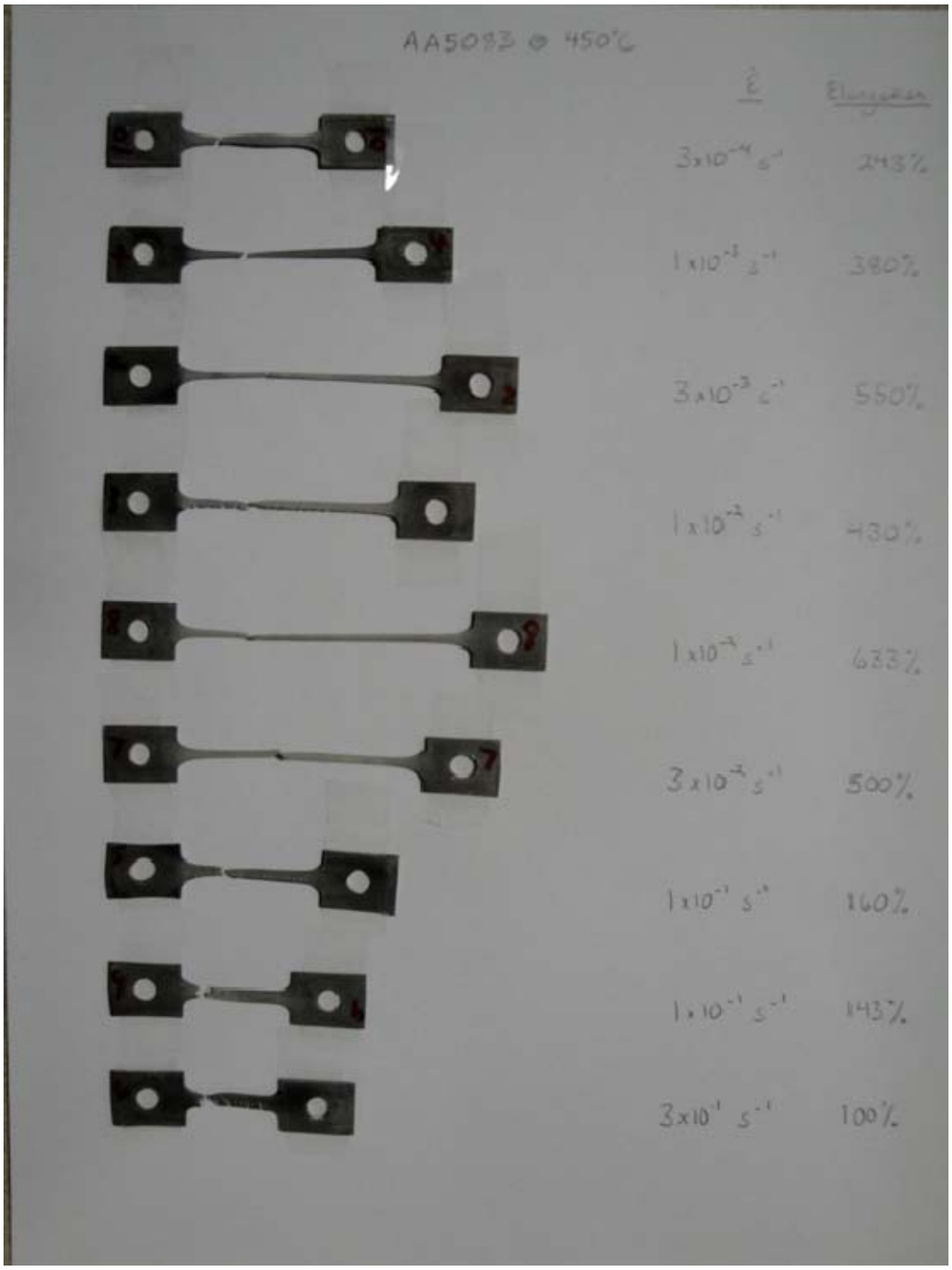

Figure 23. Tensile samples of FS processed AA5083 after being pulled to failure at 450ºC. The samples tested at the lowest strain rate are at the top and the largest strain rates are at the bottom of the picture. A maximum elongation of 633% was achieved.

A maximum elongation of 663% was achieved at a strain rate of 1 x 10^{-2} s^{-1}. Most of the samples experience superplastic behavior, except for the three samples tested at higher strain rates (≥1 x 10^{-1}). These samples did not elongate past 200% of their original length. A plot of the data showing the variation in elongation with strain rate is given in Figure 24.

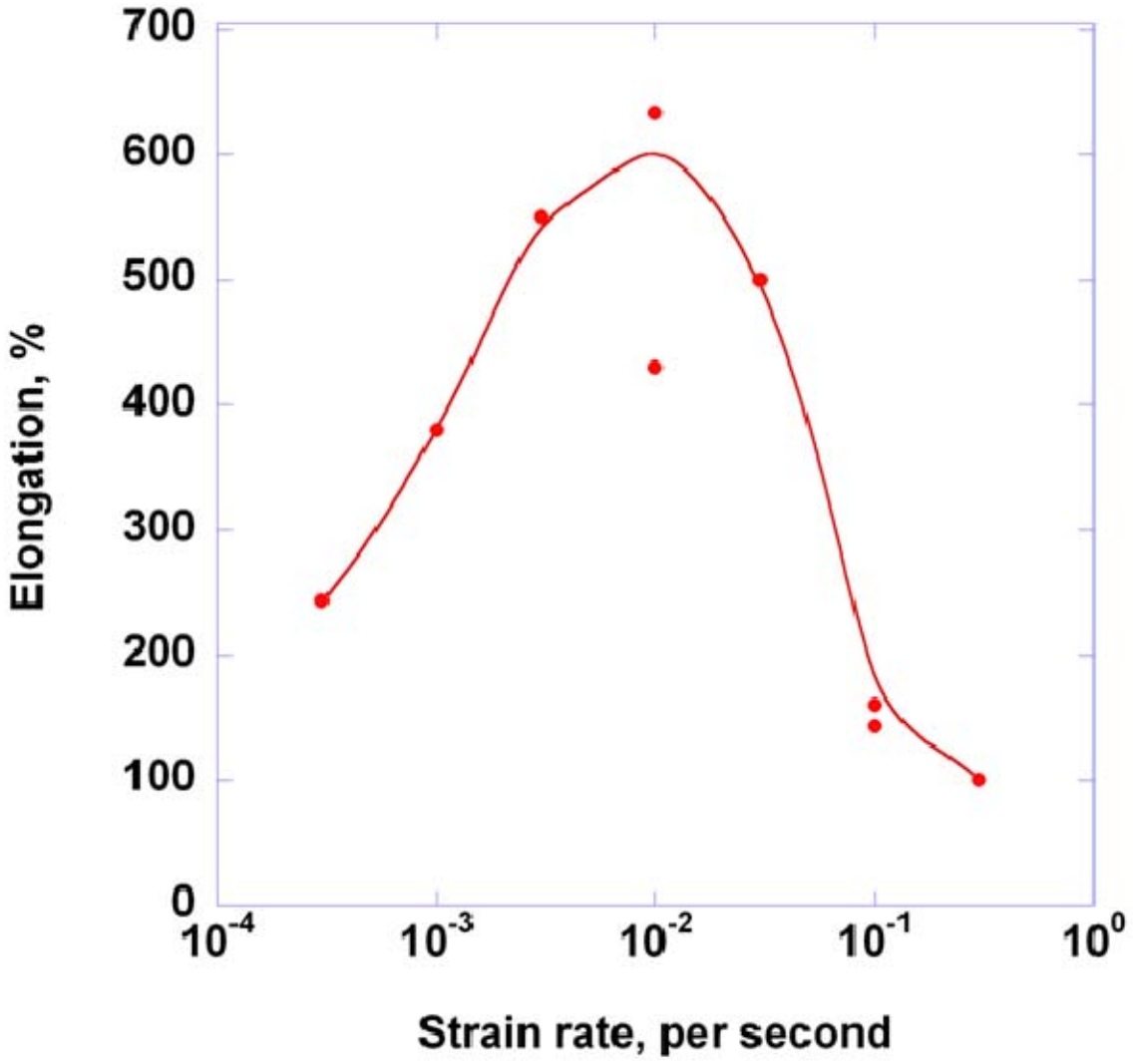

Figure 24. Graph showing the variation of elongation with strain rate. The graph shows an increase in elongation with an increase in strain rate to 1 x 10^{-2} s^{-1}. Then, the elongation decreases past strain rates of 1 x 10^{-2} s^{-1}. A maximum elongation occurred at 1 x 10^{-2} s^{-1}.

Stress-strain curves were not obtained in this study due to the use of a large load cell to pull the samples to failure. The amount of force needed to pull the sample to failure was an order of magnitude smaller than the maximum force put out by the load cell. This disparity did not allow for the sensitivity needed to create a meaningful stress-strain curve. This also prevented the obtainment of true strain values.

E. COMPARISONS WITH OTHER WORK

Similar work had been completed on the superplastic behavior of FS processed AA5083. Figure 25 provides a comparison of previous work with the results obtained in this study.

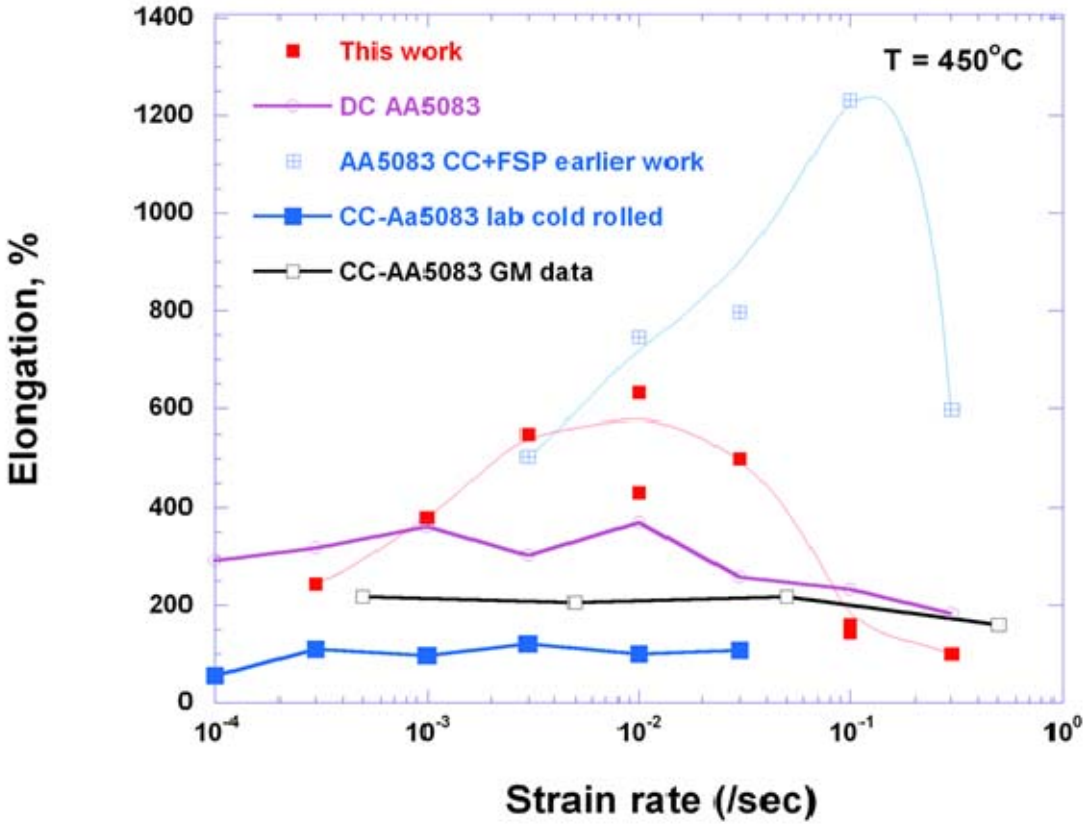

Figure 25. Elongation behavior achieved under various processing conditions. (a) FSP at 800 rpm and 76.2 mm min^{-1} (b) DC AA5083 (c) FSP at 350 rpm and 101.6 mm min^{-1} (d) CC-AA5083 lab cold rolled (e) CC-AA5083 GM data. Maximum elongation of 1245% occurred in data set (c) at a strain rate of 1 x 10^{-1} s^{-1}. Trends between the two FS processed materials are similar, with the graph from this study being shifted down and to the left.

The trends between the two studies are similar, as both experience maximum elongations. However, the data obtained in this study is shifted down and to the left, meaning the maximum elongation is less and occurs at a smaller strain rate. The maximum elongation for the previous data was 1245% and occurred at a strain rate of 1 x 10^{-1} s^{-1}. The previous FS processed AA5083 was obtained by processing at 350 rpm, 101.6 mm min^{-1} and using a smooth pin. FSP created an average grain size of 2 μm. This refined grain size contributed to the exceptional elongation exhibited. The material processed in this study exhibited lower elongation at lower strain rates because the grain size achieved was larger than the previous study. However, both of the FS processed materials exhibited greater peak elongation than the other methods. This improvement in superplastic behavior can be attributed to the grain refinement in the stir zone, as well as the increase of high angle grain boundaries and the homogeneity of precipitate particles.

THIS PAGE INTENTIONALLY LEFT BLANK

V. DISCUSSION

A. MICROSTRUCTURE ANALYSIS

The microstructure analysis in this study has shown that FSP is an effective method of refining the grain size of AA5083. The grains have been refined from a size of 70 μm in the as-received, as-cast base metal to 4 μm within the stir zone. Scans of different regions within the stir showed that the grain size was quite uniform throughout the stir zone.

Several mechanisms of grain refinement during FSP have been reported. These mechanisms include dynamic recrystallization (DRX), geometric dynamic recrystallization (GDRX) and particle stimulated nucleation (PSN) [23]. This study has shown that a very fine grain structure may be produced in AA5083 by FSP. The details of the recrystallization mechanism in these microstructures are unclear. However, dynamic recrystallization likely has an important role during FSP [24] and precipitate particles certainly contribute to the formation and retention of a refined grain structure. Further research work is needed to identify the grain refinement mechanism.

Orientation imaging microscopy showed that the fine grain structures in the FS processed AA5083 consisted of mainly high angle grain boundaries. The large fraction of high angle grain boundaries make it easier for grain boundary sliding to occur, leading to superplasticity.

A weak deformation texture was found in the FSP samples. The base metal had a random texture. The weak deformation texture is persistent through the entire stir zone. It is also retained after the extended time at temperature.

An important issue when dealing with processing parameters is the heat input to the work piece. By varying the two processing parameters of tool rotation rate and traversing rate, the peak temperature reached in the work piece can be altered. Decreasing the tool rotation rate or increasing the traverse rate will decrease the heat input. This will lead to a smaller grain size. A smaller grain size should result in better superplastic behavior. This assertion is backed up the comparisons of the AA5083 processed in this

work and the AA5083 processed in the earlier study by Bland [16] wherein the plate was processed at slower tool rotation rates and a faster traverse rate. The resulting average grain size was smaller than the grain size in this work. The smaller grain size was a factor in longer elongations observed.

The stir zone for the AA5083 processed in this study was intact and free of any macroscopic defects. While the appearance of a tunnel defect does not appear to have any impact on the superplastic behavior, it should be noted that an intact stir zone is more desirable.

Post-processing annealing at 450ºC had very little effect on the average grain size within the processed zone. These results show that the grain growth is stable throughout the tensile testing process. Stable grain growth eliminates abnormal grain growth during the tensile testing. Abnormal grain growth often occurs in FSP materials and is characterized by an exponential growth in grain size due to a prolonged exposure to high temperature.

The homogeneous precipitate particle distribution is also a large factor in the superplastic behavior of the FSP AA5083. The particles within the stir zone are much finer than the particles found in the as-cast material. The more uniform particle distribution contributes to the improved mechanical properties of the material.

B. MECHANICAL PROPERTIES ANALYSIS

The superplastic testing conducted in this research shows that FSP was an effective method for creating elongations over 200%. The increased ductility in the FSP AA5083 materials is most likely due to several factors, with the most prominent being the grain refinement. The small grains make it difficult for dislocations to move, thus increasing the yield strength of the material. The small grain size enables the deformation of the material by grain boundary sliding, allowing the material to stretch superplastically. The homogeneity of the precipitate particles delays void nucleation and cavitation growth within the material, thereby delaying the failure mechanism. Also, the large fraction of high angle grain boundaries allows for the grain boundaries to slide, thus enhancing the plastic behavior of the material.

VI. CONCLUSIONS

1. This study successfully processed AA5083 using the FSP technique. A milling machine with a threaded pin was used to FS process the material. The parameters used were a tool rotation rate of 800 rpm, a traverse rate of 76.2 mm min^{-1} and a step-over distance of 2 mm. A high quality processed material, free of processing defects, was obtained.

2. Friction stir processing is an effective method for grain refinement in as-cast AA5083. It can be seen that the stir zone is distinct from the base metal. A grain reduction from 70 μm in the base metal to 4 μm in the stir zone was measured. The grains are equiaxed and appeared uniform throughout the stir zone. A range in grain size from 1 to 5 μm was observed in the processed material.

3. The OIM analysis showed that the fine grain structure had mainly high angle boundaries. The percentage of high angle boundaries was increased from 65% in the base metal to 80% in the processed region. The increase of high angle boundaries promotes superplastic behavior.

4. Compared with a random texture found in the base metal, the (001) pole figures suggest a weak deformation texture in the FS processed material. This texture is retained even after annealing for 240 minutes at 450ºC.

5. The base material shows large concentrations of precipitate particles. After FSP, the precipitates were refined and redistributed in a basically homogeneous manner throughout the stir zone. The homogeneous particle distribution also contributes to superplastic behavior.

6. The annealing procedure shows that stable grain growth takes place in the FS processed AA5083. This shows that no abnormal grain growth occurs in the sample during mechanical testing. Stable grain growth takes place for all of the strain rates tested.

7. The FS processed AA5083 exhibited excellent superplastic behavior at an elevated temperature of 450ºC. A maximum elongation of 633% was obtained at a strain rate of 1 x 10^{-2} s^{-1}. Superplasticity was obtained at strain rates ranging from 3 x 10^{-4} to 3 x 10^{-2} s^{-1}.

VII. RECOMMENDATIONS FOR FUTURE WORK

A. FRICTION STIR PROCESSING PARAMETERS

The processing parameters for AA5083 can be changed in order to achieve optimum processing conditions. By changing the tool rotation rate and/or the traverse rate, the amount of heat input to the work piece can be modified. The change in heat input to the work piece can be modified. The change in heat input will change the size of the grains in the stir zone. While a small microstructure is desired, the parameters must be modified to ensure that no macroscopic defects are present in the material. This may be accomplished by changing the parameters or examining the effects of the threaded pin under similar conditions. Finally, an optimized overall processing speed must be investigated if FSP is to become an economical method of producing a superplastic material. In order to minimize the processing time, yet ensuring that the entire volume of material is processed, the step-over distance needs to be optimized.

B. MECHANICAL TESTING CONDITIONS

The range of conditions under which the FSP AA5083 was mechanically tested needs to be expanded to more thoroughly evaluate the temperature and strain-rate dependence of the superplastic behavior. This would include varying the testing temperature for as-processed material as well as after various post-processing treatments to control microstructure.

THIS PAGE INTENTIONALLY LEFT BLANK

LIST OF REFERENCES

[1] The Welding Institute, *TWI Services to Friction Processing*. Retrieved December 2008, from http://www.twi.co.uk/.

[2] R. Dean, "Aluminum-Large Aluminum Extrusion in Marine Applications." *Materials World*. Vol. 3, pp. 65-67, 1995.

[3] J. Hoeven, "A New 5xxx Series Alloy Developed for Automotive Applications." *SAE International*. Doc. 2002-01-2128, July 2002.

[4] J.G. Schroth. "General Motors' Quick Plastic Forming Process." *Advances in Superplasticity and Superplastic Forming*, pp. 9-20. 2004.

[5] P.E. Krajewski: in *Advances in Superplasticity and Superplastic Forming*, E.M. Taleff, P.A. Friedman, P.E. Krajewski, R.S. Mishra, and J.G. Schroth, eds., TMS, Warrendale, PA, 2004, pp. 173-83.

[6] M.A. Kulas, W.P. Green, E.M. Taleff, P.E. Krajewski, and T.R. McNelley: *Metallurgical Materials Transactions. A*, 2005, vol. 36A, pp. 1249-61.

[7] E.M. Taleff, W.P. Green, M.A. Kulas, T.R. McNelley, and P.E. Krajewski: *Mater. Sci. Eng. A*, 2005, vols. 410-411, pp. 32-37.

[8] W.P. Green, M.A. Kulas, A Niazi, K. Oh-ishi, E.M. Taleff, P.E. Krajewski, and T.R. McNelley: *Metall. Mater. Trans. A*, 2006, vol. 37A, pp. 2727-28.

[9] T.R. McNelley, K. Oh-ishi, A.P. Zhilyaev, S. Swaminathan, P.E. Krajewski, and E.M. Taleff. "Characteristics of the Transition from Grain-Boundary Sliding to Solute Drag Creep in Superplastic AA5083." *Metallurgical and Materials Transactions A*. 2008, vol. 39A, pp. 50-64.

[10] T.R. McNelley, D.J. Michel, and A. Salama: *Scripta Metall.*, 1989, vol. 23, pp. 1657-62.

[11] E.M. Taleff: in *Advances in Superplasticity and Superplastic Forming*, E.M. Taleff, P.A. Friedman, P.E. Krajewski, R.S. Mishra, and J.G. Schroth, eds., TMS, Warrendale, PA, 2004, pp. 85-94.

[12] E.M. Taleff, G.A. Henshall, T.G. Nieh, D.R. Lesuer, and J. Wadsworth: *Metall. Mater. Trans. A*, 1998, vol. 29A, pp. 1081-91.

[13] E.M. Taleff, P.J. Nevland, and P.E. Krajewski: *Metall. Mater. Trans. A*, 2001, vol. 32A, pp. 1119-30.

[14] L.D. Hefti "Commercial Airplane Applications of Superplastically Formed AA5083 Aluminum Sheet." *Journal of Materials Engineering and Performance*. Vol. 16 (2), pp. 136-141, April 2007.

[15] R.S. Mishra. and I. Charit, "Evaluation of microstructure and superplasticity in friction stir processed 5083 Al alloy." *Journal of Materials Research*. Vol. 19 (11), pp. 3329-3342, November 2004.

[16] M.T. Bland, *Investigation of Superplastic Behavior In FSP 5083 Aluminum Alloy*, Master's Thesis, Naval Postgraduate School, Monterey, CA, June 2007.

[17] M.A. Garcia-Bernal, R.S. Mishra, R. Verma. and D. Hernandez-Silva, "High strain rate superplasticity in continuous cast Al-Mg alloy prepared via friction stir processing." *Scripta Materialia.* Vol. 60 (2009), pp. 850-853.

[18] S. Tang, *Mechanics of Superplasticity*. New York: Robert E. Krieger Publishing, 1979. T.G. Nieh, J. Wadsworth, and O.D. Sherby, *Superplasticity in metals and ceramics*. New York: Cambridge University Press, 1997.

[19] US Patent 6,712,916- Metal superplasticity enhancement and forming process. March 2004.

[20] A. Joshi. "Introduction to Superplastic Forming Process." Indian Institute of Technology, Bombay, India. November 2002.

[21] J.-Q. Su, T.W. Nelson and C.J. Sterling, "Grain refinement of aluminum alloys by friction stir processing." *Philosophical Magazine.* Vol. 86 (1), pp. 1-24, January 2006.

[22] R.S. Mishra. and Z.Y. Ma, "Friction stir welding and processing." *Material Science and Engineering R.* Vol. 50 (2005), pp. 1-78.

[23] J.-Q. Su, T.W. Nelson and C.J. Sterling, "Microstructure evolution during FSW/FSP of high strength aluminum alloys." *Materials Science and Engineering*. Vol.50 (2005), pp. 277-286.

[24] T.R. McNelley, S. Swaminathan and J.-Q. Su, "Recrystallization mechanisms during friction stir welding/processing of aluminum alloys." *Scripta Materialia*. Vol. 58 (2008), pp. 349-354.

INITIAL DISTRIBUTION LIST

1. Defense Technical Information Center
   Ft. Belvoir, Virginia

2. Dudley Knox Library
   Naval Postgraduate School
   Monterey, California

3. Engineering and Technology Curricular Office, Code 34
   Naval Postgraduate School
   Monterey, California

4. Professor Terry R. McNelley, Code ME/Mc
   Naval Postgraduate School
   Monterey, California

5. P. J. Krajewski
   General Motors Research Laboratory
   Warren, Michigan

6. E. M. Taleff
   Department of Mechanical Engineering-University of Texas at Austin
   Austin, Texas

7. Professor Jianqing Su
   Naval Postgraduate School
   Monterey, California

8. Professor Sarath Menon
   Naval Postgraduate School
   Monterey, California

9. Ensign John Hayashi
   Naval Postgraduate School
   Monterey, California